PhD

PROGRAM IN TRANSLATIONAL

AND MOLECULAR MEDICINE

DIMET

UNIVERSITY OF MILANO-BICOCCA

SCHOOL OF MEDICINE AND FACULTY OF SCIENCE

Pathophysiology of the late sodium current: from myocardium to pancreatic beta cells.

Riccardo Rizzetto

Coordinator: Prof. Andrea Biondi

Tutor: Prof. Antonio Zaza

XXV CYCLE

ACADEMIC YEAR

2012-2013

..and now, what do you plan to do?

Believe in the future,
and persist in the present

- *Firion, to Matheus*

TABLE OF CONTENTS

CHAPTER 1 - INTRODUCTION

The late sodium current (I_{NaL})

In excitable cells the sodium current (I_{Na}) is defined as the sodium flux that flows through voltage-gated sodium channels (VGSC). In muscles and neurons I_{Na} can be divided in two components: a fast activating and quickly inactivating one, commonly referred as transient I_{Na} (I_{NaT}), and a steady-state activated component (Late I_{Na}, I_{NaL}). Like the other voltage gated ion channels, the dual nature of I_{Na} is the direct consequence of the VGSC gating. The steady-state activated portion of I_{Na} can be further divided in two main components: 'true' I_{NaL} and window currents (I_{NaW}), which have been established as distinct phenomena[1;2]. I_{NaW} occurs only in a small range of membrane potentials (V_m), where the opening probability and the availability of VGSCs are both different from 0, thus allowing steady-state Na^+ influx.[1] On the other hand I_{NaL} is present in a different range of potentials which is broader than I_{NaW}; such an evidence has provided a more accurate definition of I_{NaL}, now accepted as the result of an intrinsic instability of the inactivated state of the channels[1]. According to this model, I_{NaL} results from channel reopening during sustained depolarization by two different modes, burst openings and scattered late openings (Fig. 1.1). The burst opening mode undergoes slow but complete voltage-dependent inactivation and quickly deactivates upon repolarization. On the other hand, scattered late openings inactivate very slowly and may include a non-inactivating component, which supports, in terms of macroscopic current, a truly steady-state or "background" I_{Na}[3].

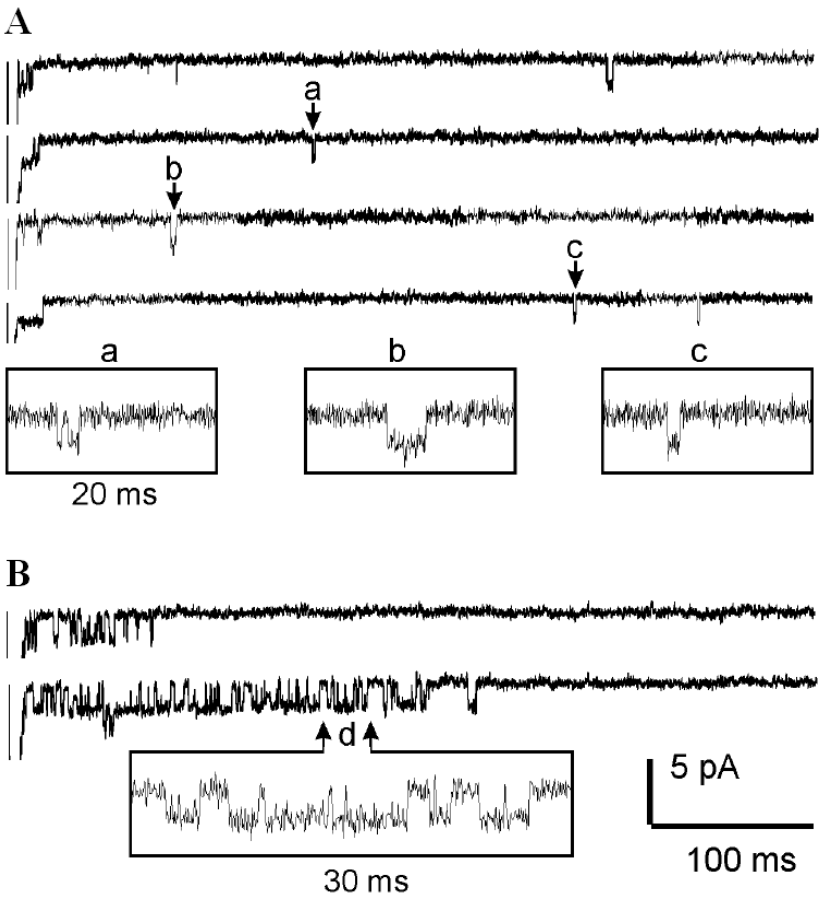

Figure 1.1. $I_{NaL.}$ ***S****ingle channel recordings showing the scattered late* ***(A)*** *and the burst* ***(B)*** *component of the late sodium current.*

Under normal conditions the entity of I_{NaL} is very small compared to I_{NaT} (less than 1%), thereby limiting its impact on the normal cellular physiology. However, an enhancement of I_{NaL} has been recently found in several heart and neurological disorders, *eg* relative ischemia[4-6], cardiac hypertrophy/heart failure [5;7], ischemia/reperfusion damage[8] and epilepsy[9]. These evidences of I_{NaL} involvement in several diseases raised the clinical interest of its blockade as an effective therapeutic tool.

Pathophysiology of I_{NaL}

Since I_{NaL} enhancement was firstly linked to relative ischemia conditions (*angina*)[10], cardiac myocytes have been intensively studied as subjects of I_{NaL}-induced damage. After the first findings regarding *angina pectoris*, I_{NaL} enhancement has also been reported in several other heart disease, including LQT-3 and LQT-4 syndromes[9;9;11;12], heart failure[5;13-15], ischemia-reperfusion damage[16;17], atrial fibrillation[18;19] and post-myocardial infarction remodeling[20].

In cardiac myocytes I_{Na} is the key element regulating action potential (AP) upstroke and signal conduction from the sinoatrial node to the ventricular chambers; however, since I_{NaL} is very small in normal conditions, the physiological role of I_{Na} is almost carried out by I_{NaT}.

Besides genetic mutations affecting directly the VGSC gating[21;22], several other conditions common in cardiac disease, like reactive oxygen species (ROS), hypoxia or ischemic metabolites, are strong enhancers of I_{NaL}[16;17;23]. Such an increase may have at least two functional consequences: electrical instability and ionic homeostasis derangements.

The former is due to the impact of I_{NaL} on ventricular repolarization dynamics, which in turn are tightly coupled with the action potential shape (Fig. 1.2). In ventricular myocytes APs are evoked by the simultaneous opening of VGSCs, triggering a fast depolarization mostly driven by I_{NaT} (Phase 0). After this initial phase, I_{NaT} inactivates and the opening of K^+ conductances (I_{to}) starts the repolarization process (Phase 1). The repolarization is partially counteracted by Ca^{2+} entry via the L-type Ca^{2+} current (I_{CaL}), leading to the typical 'plateau' (phase II) responsible for the Ca^{2+} influx

necessary for systolic contraction. The subsequent shift of the balance between inward (I_{CaL} and I_{NaL}) and outward (K^+) currents leads to the final repolarization (Phase 3) and diastole (Phase 4).

I_{NaL} is present throughout the repolarization process (mainly Phase 2 and 3), but its impact on the AP is negligible in normal conditions[1]. However, in the presence of I_{NaL} enhancement, the higher inward current during the plateau leads to an abnormal prolongation of the AP duration (APD)[2;22].

The longer APD can reactivate Ca^{2+} channels, producing abnormal and proarryhthmic depolarizations (early afterdepolarizations, EADs)[24;25]. Moreover, I_{NaL} enhancement leads to intracellular Na^+ accumulation during the systole, altering the function of the Na/Ca exchanger (NCX). Since diastolic potential (Phase 4) is dependent from the balance between NCX activity and the K^+ current I_{K1}[26], an increase in systolic Ca^{2+} will facilitate the forward mode of NCX in diastole, thus providing depolarizing current responsible for delayed afterdepolarizations (DADs) and triggered activity[26-28]. Therefore an enhancement of I_{NaL} can trigger both EADs and DADs, leading to spontaneous arrhythmias and ventricular fibrillation[2;28-31].

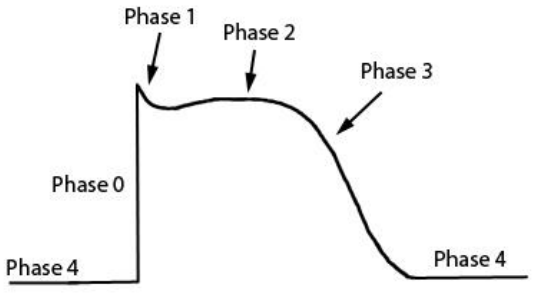

Fig. 1.2 Ventricular action potential.

The second effect of I_{NaL} enhancement is directly linked to the abnormal Na^+ entry for a longer period of time (caused by APD prolongation), which leads to intracellular Na^+ accumulation. This alters the normal extrusion of Ca^{2+} via NCX, with the net result of intracellular Ca^{2+} (Ca_i) overload[2;32]. Keeping high levels of Ca^{2+} may be a compensatory mechanism during systole in cases of afterload increase, but defects of Ca^{2+} removal may jeopardize myocardial relaxation during diastole and ultimately leads to diastolic dysfunction[14;17]. Moreover, Ca_i is a critical factor for several intracellular pathways, including gene expression and apoptosis[33-38]. Indeed Ca^{2+} overload is the common feature shared by all heart disease and it is tightly linked to ventricular remodelling, the process of progressive and detrimental changes in ventricular myocytes gene expression and function [34;36;39-42]. It has been reported that both Ca^{2+} overload and its negative effects are reduced by I_{NaL} blockade (Fig. 1.3)[8;14;17;21;43;44].

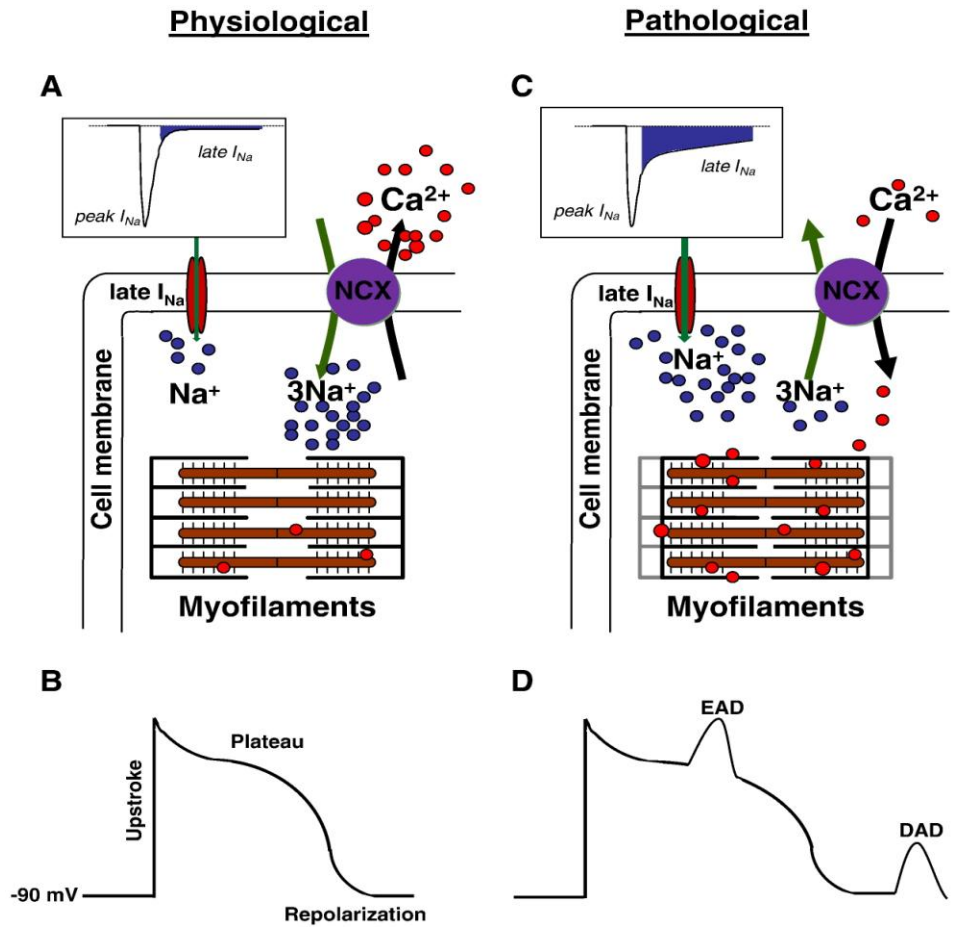

Fig. 1.3 Functional impact of I_{NaL}. *Representative scheme of a ventricular myocyte during physiological (**A** and **B**) and pathological (**C** and **D**) conditions. Note the presence of both ionic (Ca^{2+} overload) and electrical (proarrythmic EADs and DADs) derangements in panels **C** and **D**.*

It has been recently demonstrated that in failing myocytes I_{NaL} and Ca^{2+} overload are interconnected by a loop, in which high levels of Ca^{2+} activate the Ca/calmodulin-dependent protein kinase CaMKII[43;45], that in turn phosphorylates the Na^{+} channel, thus enhancing I_{NaL} and closing the loop[46]. However, the evidence that Na^{+} accumulation precedes Ca^{2+} overload[47] suggests I_{NaL} as the most promising therapeutic target for interrupting this loop.

Pharmacology of I_{NaL}

As expected from its nature, I_{NaL} is inhibited by common Na^+ channel blockers (*eg,* TTX, Cd^{2+}, lidocaine). However the common drugs affecting VGSC don't discriminate between I_{NaT} and I_{NaL}, thus hampering their effectiveness in clinical practice.

Nevertheless, the increasing evidence of I_{NaL} involvement in congenital and acquired disease has promoted the research for a selective blocker of I_{NaL} over its transient counterpart. Ranolazine (RAN), a piperazine derivative approved by FDA as an antianginal drug[10;48;49], is the drug already available in clinic with the most selectivity for I_{NaL}. (IC_{50} for I_{NaL}/IC_{50} for I_{NaT}: 37.8[13]).

Despite the fact that RAN is also an aspecific blocker of the rapid delayed rectifier current I_{Kr} at therapeutic concentrations (IC50 for I_{Kr}: 12 μM)[50],several groups demonstrated its efficacy as selective I_{NaL} blocker in conditions where I_{NaL} was induced by ischemia or pharmacological agents (*ie* ATX II)[17;51].

It has also been shown that I_{NaL} blockade by RAN was effective in reducing diastolic cell Ca^{2+} accumulation in chronic heart failure[14] and in preventing ischemia-reperfusion injury[52]. Moreover, it has been shown that I_{NaL} blockade has beneficial effects in human hypertrophic cardiomyopathy[7].

Starting from this experimental evidences, several clinical trials tested RAN for the treatment of a wide spectrum of pathologies[4;6;53]. These clinical trials demonstrated the beneficial effects of RAN in stable angina when used alone (Monotherapy Assessment of Ranolazine in Stable Angina, MARISA)[53] or associated with other commonly used

drugs (Combination Assessment of Ranolazine in Stable Angina, CARISA)[4].

The MERLIN-TIMI 36 clinical trial was designed to test the effectiveness of the extended-release formulation of RAN in patients with acute coronary syndrome (ACS) and demonstrated a significant reduction in the incidence of recurrent ischemia after the therapy[54]. However, addition of RAN to the standard treatment for ACS was not effective in reducing major cardiovascular events[54].

Despite its cardiac action, it has been shown from *in vitro* experiments that RAN is not selective for the cardiac VGSC isoform ($Na_V1.5$), but the drug can interact with other isoforms, including the TTX-sensitive $Na_V1.7$[55], $Na_V1.4$[56] and the TTX-resistant $Na_V1.8$ channels[55]. Since these VGSC isoforms are expressed mostly in systems different from the heart (*ie* DRG neurons[57] or skeletal muscles[56]), ancillary effects of RAN might be expected.

During the MERLIN-TIMI 36 clinical trial, it has been reported that chronic treatment with RAN had an unexpected, albeit important, beneficial effect in reducing glycosylated haemoglobin levels in type II diabetic patients[58]. Further studies on the streptozotocin (STZ)-induced diabetes animal model demonstrated an improvement of glucose homeostasis in mice treated with RAN because of increased insulin secretion from pancreatic islets, subsequent to prevention of β-cell apoptosis[59]. These multiple evidences suggest that I_{NaL} may be involved in the insulin secretion process, thus opening a new potential therapeutic target for type II diabetes.

Type II diabetes mellitus

Diabetes mellitus (DM) is a widespread pathology with multiple etiology characterized by defection in insulin secretion[60], insulin action[61] or both. In 2012 it was the most common endocrine disorder, affecting about 5% of the world's population[62]. The general hallmark of DM is chronic hyperglycemia, associated with disturbances in carbohydrates, fat and protein metabolism.

Traditionally DM has been divided into two major subtypes:

- Type I DM (T1DM) is characterized by pancreatic β cell destruction, with little or no endogenous insulin secretory capacity. Because of its genetical cause, it is the less common type of DM (5-10% of all new cases of diabetes) and it is usually referred as an autoimmune disease[63].
- Type 2 DM (T2DM) is often recognized as 'late onset' diabetes, characterized by peripheral insulin resistance and β-cell dysfunction. It accounts for over 90% of all new cases of diabetes, thus it is the most frequent disorder in clinical practice[63].

Besides these two major classifications, other subtypes of DM, as the pregnancy diabetes or specific genetic defects, complete the state of the art of the pathology[63]. (Table 1)

Type I diabetes (β-cell destruction, usually leading to absolute insulin deficiency)
- A. Immune mediated
- B. Idiopathic

II. Type II diabetes (may range from predominantly insulin resistance with relative insulin deficiency to a predominantly secretory defect with insulin resistance)

III. Other specific types
- A. Genetic defects of b-cell function
  1. Chromosome 12,HNF-1α (MODY3)
  2. Chromosome 7, glucokinase (MODY2)
  3. Chromosome 20, HNF4α (MODY1)
  4. Chromosome 13, insulin promoter factor-1 (IPF-1, MODY4)
  5. Chromosome 17, HNF-1β (MODY5)
  6. Chromosome 2, *NeuroD1* (MODY6)
  7. Mitochondrial DNA
- B. Genetic defects in insulin action
  1. Type A insulin resistance
  2. Leprechaunism
  3. Rabson-Mendenhall syndrome
  4. Lipoatrophic diabetes
- C. Diseases of the exocrine pancreas
  1. Pancreatitis
  2. Trauma/pancreatectomy
  3. Neoplasia
  4. Cystic fibrosis
  5. Hemochromatosis
  6. Fibrocalculous pancreatopathy
- D. Endocrinopathies
  1. Acromegaly
  2. Cushing's syndrome
  3. Glucagonoma
  4. Hyperthyroidism
  5. Somatostatinoma
  6. Aldosteronoma
  7. Others
- E. Drug- or Chemical-induced
  1. Vacor
  2. Pentamidine
  3. Nicotinic acid
  4. Glucocorticoids
  5. Thyroid hormone
  6. Diazoxide
  7. β-adrenergic agonists
  8. others
- F. Infections
  1. Congenital rubella
  2. Cytomegalovirus
  3. Others
- G. Uncommon forms of immune-mediated diabetes
  1. 'Stiff-man' syndrome
  2. Anti-insulin receptor antibodies
- H. Other genetic syndromes sometimes associated with diabetes
  1. Down's syndrome
  2. Klinefelter's syndrome
  3. Turner's syndrome
  4. Others

IV. Gestational diabetes

Table 1: Classification of diabetes based on its etiology

Adapted from American Diabetes Association[63]

T2DM is the most common type of diabetes[64]; it is a complex heterogeneous group of metabolic conditions, thus involving almost all tissues and organs in the human body[64]. The involvement of each tissue or organ to T2DM is summarized in Fig. 1.4. Current theories on T2DM include a defect in insulin-mediated glucose uptake by skeletal muscle, a disruption of secretory function of adipocytes, a dysfunction of pancreatic β cells, impaired response to hyperglycemia in the central nervous system and impaired fatty acid oxidation due to obesity or genetic predisposition[64]. However, since insulin is the hormone mainly involved in glycaemic control, one of the main focus in treating T2DM is targeting the insulin secretion process in pancreatic β cells. Indeed many mechanisms contributing to T2DM may trigger β cell apoptosis[65] and reduce β cell mass or ability to compensate for insulin resistance[66].

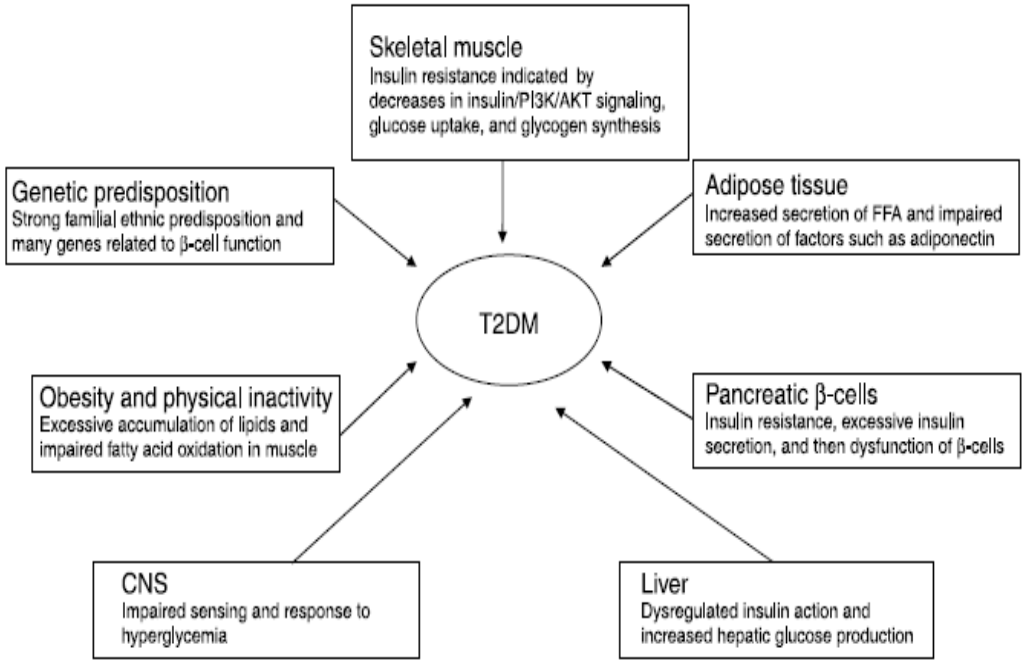

Fig. 1.4 Pathophysiology of T2DM. *Adapted from Lin et al*[62]

Physiology of insulin secretion

Insulin is a peptide of 51 aminoacids, with a molecular mass of 5,8kDa . Functional insulin consists of two polypeptide chains, A- and B-chain, linked together by disulphide bonds.
The synthesis of insulin (Fig. 1.5) occurs in pancreatic β-cells and is independent from blood glucose levels. The initial product deriving from insulin gene expression is a longer peptide, named preproinsulin. Preproinsulin contains a 24 aminoacids signal peptide, which acts as a cleavage signal for endoproteases. After this initial cleavage, proinsulin is formed. This new polypeptide undergoes subsequent cleavage and the disulphide bonds between A- and B- chain are formed, thus producing 'final' insulin and the residual C-peptide. C-peptide itself is a functional polypeptide, as it is used to treat T1DM-derived disorders[66-69]. Insulin is stored as hexamers containing Zn^{2+} ions in vesicles present in the cytosol of pancreatic β cells. After secretagogue stimuli (*eg* high plasma glucose levels) promote granules exocytosis, insulin secretion occurs.

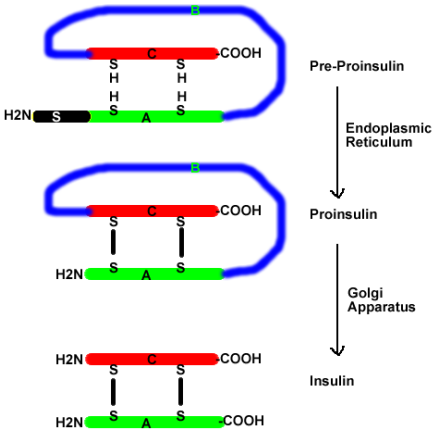

Fig. 1.5 Insulin biosynthesis

The glucose-stimulated insulin secretion (GSIS) from pancreatic islets occurs in two phases: the first, lasting 5-10 minutes, is largely dependent on membrane electrical activity, whereas the second is longer (up to hours) and involves several metabolic pathways.

The first phase of GSIS is commonly referred as the 'K_{ATP}-channel dependent pathway', because of the central role of I_{KATP} in triggering the response. (Fig. 1.6) In low glucose conditions, K_{ATP} channels are constitutively open, thus maintaining the β cell in a hyperpolarized state. Following glucose metabolism, the ATP/ADP ratio increases and the K_{ATP} channels close, thus leading to membrane depolarization. Voltage-dependent Na^+ and Ca^{2+} channels (respectively VGSC and VGCC) open in response to this initial depolarization, starting oscillatory electrical activity characterized by burst of action potentials[70]. The final result is an increase in intracellular Ca^{2+}, which in turn triggers exocytosis of insulin granules.

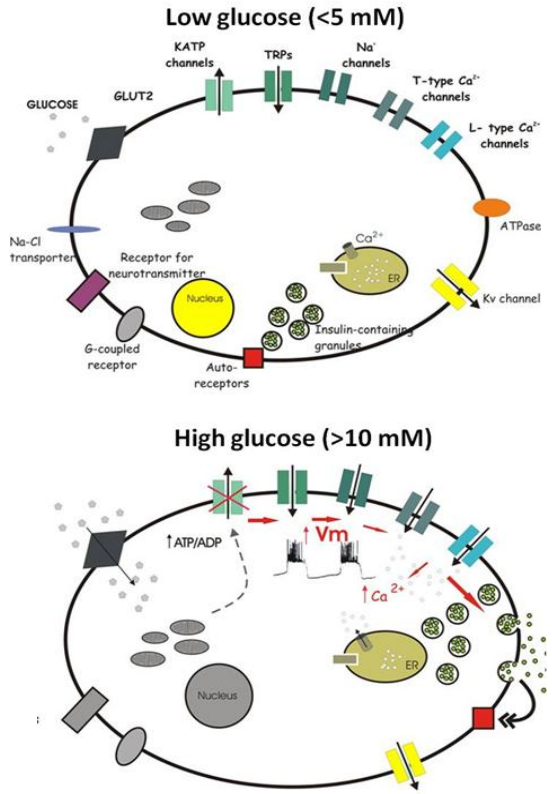

Fig. 1.6 First phase of insulin secretion.

Schematic representation of a pancreatic β cell under resting (low glucose, up) and stimulated (high glucose, below) conditions.

Besides this traditional pathway, it has been proposed a second mechanism underlying the first phase of insulin secretion, named 'the VRAC hypothesis' [71]. According to this theory, the accumulation of glucose metabolites leads to an increase of solutes in the β cell cytosol, thus producing cell swelling. The increase in volume of the cell leads to the opening of a volume-regulated anion channel

(VRAC), which mainly drives a putative Cl^- conductance responsible for membrane depolarization and Ca^{2+} entry via VGCC[70]. This mechanism has been proposed as an ancillary pathway other than the classic K_{ATP}-dependent pathway[70], and it may account for the presence of insulin secretion in β-cells exposed to high glucose levels in the presence of the K_{ATP} channel opener diazoxide[72]. However, glucose-induced cell swelling is not present in every pancreatic β cell model[72;73], suggesting that the VRAC hypothesis may account for some insulin secretion only in particular conditions.

Regardless the mechanisms that drive membrane depolarization, the latter is a crucial component for Ca^{2+} entry, necessary for the first phase of GSIS. In mouse β cells, studies on the molecular machinery involved in insulin exocytosis identified synaptotagmin-7 (Syt7) as the main Ca^{2+} sensor for the process[74]. In humans the Ca^{2+} sensor is represented by both Syt7 and Syt5 proteins, which are the ultimate molecular transducers before the first-phase exocytosis[75].

On the other hand, the second phase of GSIS is dependent from different intracellular signalling pathways. It has been demonstrated that this phase is not strictly dependent from intracellular Ca^{2+} and requires high glucose in the extracellular environment[72]. Other intracellular pathways include long chain acyl-CoA molecules[76-78], direct ATP interaction with secretory granules[79], c-AMP levels modulation[80;81], protein kinase A (PKA)[82] and protein kinase C (PKC)[81] activation.

Insulin secretion from pancreatic β-cells can be activated by several secretagogues other than glucose. Charged aminoacids, like arginine, can enter the cell and trigger depolarization of the cell membrane, thus

promoting Ca^{2+}-dependent exocytosis of insulin granules[83]. Fatty acids may enhance insulin secretion by both mitochondrial (beta-oxidation) and cytosolic (direct signalling on exocytosis) mechanisms[77;78;84].

Besides nutrients, other molecules, like neurotransmitters[85], and hormones[86;87] may affect insulin secretion. A crucial role is played by paracrine signals in the entire islet[88]. Indeed, glucagon produced by the neighbouring α cells acts as strong enhancer of insulin secretion[89], while somatostatin (produced by δ cells) is a known inhibitor of the process[89;90]. Since pancreatic β-cells express the insulin receptor, insulin itself is a strong enhancer of GSIS, giving rise to autocrine signalling[91].

Moreover, several drugs have been developed to improve insulin secretion and are used in clinic to achieve glycaemic control in T2DM. This is the case of sulfonylureas, like tolbutamide or glibenclamide, which are direct blockers of K_{ATP} channels[92;93]. The insulin response induced by sulfonylureas is general lower than the response evoked by high glucose, but still they are effective in promoting insulin secretion.

Other drugs that modulate the electrical activity of pancreatic β cells, such as K^+ channels blockers (TEA, 4-aminopyridine)[94-96] or Ca^{2+} channels activators (Bay K)[97;98], enhance the response of glucose in terms of insulin secretion. On the other hand, K^+ channel activators (*ie* diazoxide)[99] or Ca^{2+} channel blockers (nifedipine)[99-101], are well known inhibitors of insulin release[102;102;103]. Thus, these evidences emphasize the strategy of modulating electrical activity as an effective therapeutic target in the management of T2DM.

Electrophysiology of the pancreatic β cell

The electrical activity in pancreatic islets is dependent from the levels of blood glucose and has an intrinsic oscillatory nature.[70]

In low glucose (<3 mM) conditions, the β cell membrane is in a hyperpolarized state (about -70 mV) due to the presence of I_{KATP} and background currents. When the glucose levels raise, the closure of K_{ATP} channels results in a net depolarization on which spontaneous action potentials (APs), single or grouped in 'bursts', are superimposed. These V_m oscillations are coupled with the oscillations in intracellular Ca^{2+} necessary for the GSIS process (Fig. 1.7)[75].

The oscillatory nature of V_m changes evoked by glucose is a direct consequence of the subset of ion channels that underlie the electrical activity and are expressed in β cells. In humans the ion channel complements include at least four subtypes of K^+ currents (I_{KATP}, delayed rectifier, $I_{Ks,}$ I_{KCa}), several Ca^{2+} (I_{CaN}, I_{CaL} and I_{CaT}) and at least two Na^+ currents (I_{NaT} and I_{NaL})[103].

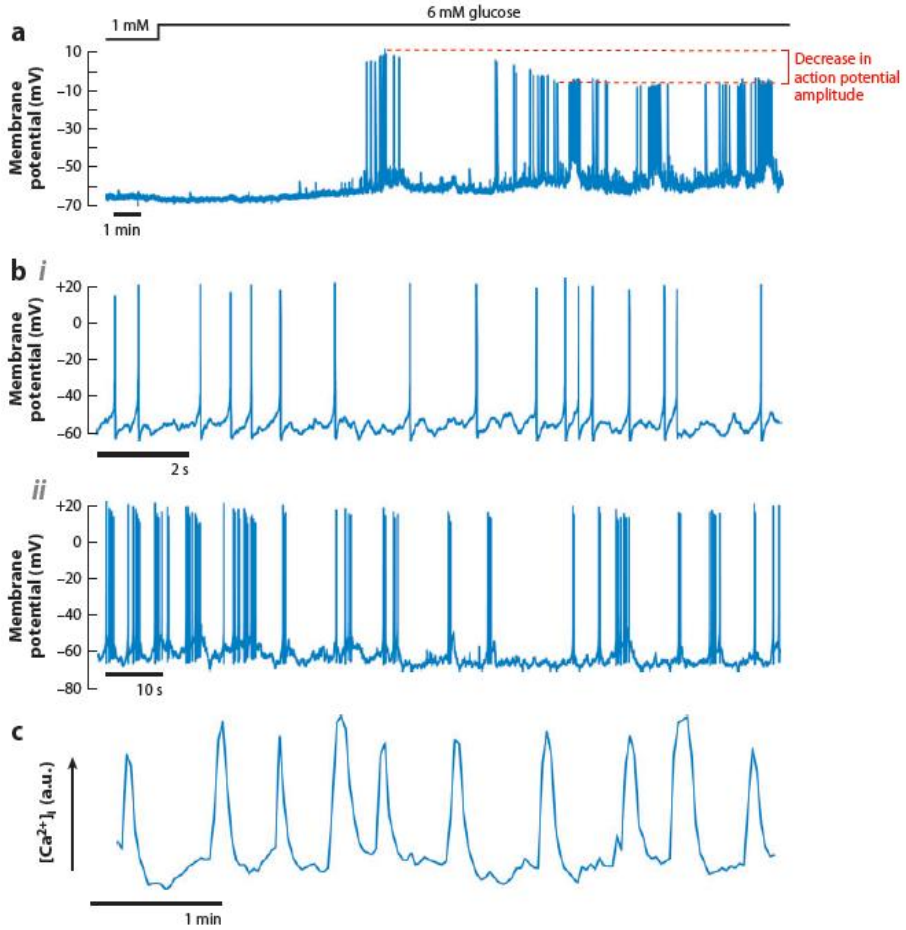

Fig. 1.7 Glucose-induced V_m and Ca^{2+} oscillations.

a *Glucose-induced V_m depolarization and initiation of electrical activity.*

b *Patterns of glucose-induced electrical activity.* i *single action potentials from a negative V_m* ii *oscillatory electrical activity*

c *Oscillatory increases of Ca^{2+} following electrical activity*

(Adapted from Rorsman and Braun)[75]

K^+ channels

The voltage-gated K^+ channels (VGKC) are tetrameric integral membrane proteins that form aqueous pores through which K^+ can flow[104]. Since K^+ currents (I_K) are normally outward, VGKCs are the main proteins involved in the repolarization of V_m in all excitable cells. A particular group of K^+ channels is represented by the inward rectifier channels (K_{IR}), which are mainly responsible for maintaining the resting V_m of particular cell types in a hyperpolarized state (*eg* I_{K1} in ventricular myocytes).

The major I_K involved in pancreatic β cell physiology is $I_{KATP,}$ whose channels belong to the K_{IR} family and are sensitive to intracellular ATP concentration. K_{ATP} channels are tetradimers composed of pore-forming subunits (K_{IR}6.x) and sulfonylurea receptor SURx, which act as regulatory subunits[105]. When ATP increases, such as after exposure to high glucose, the nucleotide binds a specific domain in the SURx sequence, causing the conformational change that drives the closure of the channel. On the other hand, when the ATP/ADP ratio drops, as in low glucose conditions, the nucleoside diphosphate displaces ATP from the SUR binding domain and the channel reopens as a result[105;106]. Since in low glucose conditions I_{KATP} is active at steady state, this current is the major controller of the membrane resting potential (-70 mV). Thus, I_{KATP} blockade has been proposed as therapeutic target to improve insulin secretion in diabetes and several drugs, like sulfonylureas, have been demonstrated to be successful in the management of T2DM[107;108]. Upon depolarization caused by K_{ATP} channel closure, the other voltage-gated ion channels open, starting the electrical activity[109].

Besides I_{KATP}, other VGKCs regulate the electrical activity of pancreatic β cells. In humans the most relevant ones are the large-conductance Ca^{2+} activated K channels (BK), the *ether-à-go-go* (hERG) and the K_V 2.2 channels.

The presence of hERG channels has been demonstrated by Rosati *et al*[110]. Addition of the selective blocker WAY- increased by 32% the firing frequency and the insulin secretion stimulated by both glucose and arginine by 70%[110]. However, since hERG channels are widely expressed throughout the central nervous system and play a major role in the repolarization of ventricular myocytes, blockade of these channels is unlikely to be used as therapeutic strategy in T2DM.

BKs are critical for the maintenance of V_m oscillations in human β cells. These channels are encoded by the KCNMA1 gene and their gating is strictly dependent from the levels of Ca_i[111]. The I_K provided by these channels can be selectively blocked by iberiotoxin. The inhibition of BK channels increases the action potential height and enhances GSIS in human β cells[103].

Moreover, blockade of BK channels unmasks a stromatoxin-sensitive delayed rectifier $I_{K,}$ that has been found to be carried by Kv 2.2. Despite the failure of stromatoxin in enhancing GSIS[103], recent evidence suggests that Kv 2.2 channels regulate exocytosis in human β cells independently of their ion-conducting function[103;112], thus keeping open the possibility of modulating these proteins as therapeutic targets.

Ca^{2+} channels

Upon glucose-induced V_m depolarization, the voltage-gated Ca^{2+} channels (VGCCs) open, providing inward currents that participate to APs generation.

Braun *et al* isolated several types of I_{Ca} in human β-cells based on their pharmacology[103]. The sensitivity of the inward currents to isradipine and NNC 55-3096 demonstrated the presence of the L- and T-type I_{Ca}, while the response to ω–agatoxin demonstrated the presence of neuronal types of I_{Ca} (P/Q and N types)[103]. Similar VGCC subtypes were identified in mice islet preparations[113;114]. It has been shown also that $Ca_V1.3$, rather than $Ca_V1.2$, is the L-type Ca^{2+} channel isoform more relevant in the stimulus secretion coupling of mice[99;100].

Since the T-type Ca^{2+} channels are low-voltage-activated (LVA), this subtype is the first to activate following I_{KATP} closure and give rise to a transient I_{Ca}, that can be isolated with the selective blocker NNC 55-3096[103]. The initial opening of I_{CaT} triggers further depolarization of V_m, allowing the activation of the high-voltage-activated (HVA) L and P/Q types VGCCs, thus enhancing the total Ca^{2+} influx into the cell.

The following rise of Ca_i triggers further release of Ca^{2+} from the intracellular stores, that is in part mediated by Ryanodine receptors (RyRs)[115], thus leading to the final rise to Ca_i necessary for GSIS.

In human pancreatic β cells, addition of selective I_{Ca} blockers slowed the spontaneous firing of APs, even stopping the electrical activity induced by 20 mM glucose[103]. Since Ca^{2+} is the main responsible for the phase I exocytosis, blockade of I_{Ca} didn't affect electrical activity only, but almost blunted GSIS[103].

Role of I_{Na} in the pancreatic β cell

The presence of VGSCs in pancreatic islets has been known since 1970[116]. The initial work about VGSCs in β-cells was controversial and concluded that I_{Na} was not involved in the spontaneous AP firing of β cells because glucose-induced electrical activity was not affected by tetrodotoxin (TTX)[117]. Subsequent studies reported that veratridine, a VGSC opener, increased insulin secretion from perfused isolated rat islets[118] and this effect was blunted by TTX. On the other hand, the VGSC activator BDF-9148 was found to be ineffective in the regulation of GSIS in mouse islets, because the drug didn't affect the electrical activity of the β cells[119]. Moreover, studies on mice lacking the regulatory β subunit of the VGSC showed that these animals have a diabetic phenotype, with both glucagon and insulin secretion impairment[120].

The first demonstration of the physiological importance of I_{Na} was made in rat β cells by Hiriart and Matteson, who also showed that this current is functionally important for stimulus-secretion coupling because TTX partially inhibited GSIS in their model[121]. TTX had no significant effect at or below 5 mM glucose, but at higher glucose concentrations TTX clearly inhibited the secretory response[121]. Further studies demonstrated that VGSCs are present and participate in GSIS by depolarizing the membrane in canine and human β-cells[122;123]. The controversial effects of TTX on GSIS of different animals were partially explained by Plant, who demonstrated that most of the VGSCs in mice β cells are inactivated at the physiological 'resting' potential, thus hampering I_{Na} impact on GSIS[124]. A recent

comparative work between mice and rat β cells showed that the percentage of VGSCs available for opening at the physiological resting potential (-70 mV) is species-specific[125]. Indeed, VGSCs expressed in rat β cells were only 50% inactivated at -70 mV, in contrast to those expressed in mice (nearly 99% inactivated)[125]. In humans the steady-state inactivation of I_{Na} is half-maximal at approximately -40 mV, thus VGSCs may be recruited to participate to AP generation until the glucose-induced depolarization exceeds this value[75]. This view is supported by the evidence that TTX inhibition of GSIS is maximal under exposure to a mild concentration of glucose (6-7 mM), while the toxin is less effective in the presence of high glucose concentration (20 mM)[103;122].

However, the impact of VGSCs on the physiology of pancreatic β cells may not be limited to the net inward current provided by $I_{Na,}$ because intracellular Na^+ levels are tightly linked to both pH and Ca_i. The former is controlled by the activity of the Na/H exchanger (NHE), that plays a major role in the protection against metabolic acidosis, but its ablation has negligible effects on GSIS[126]. However, since the activity of several anabolic enzymes is strictly dependent on pH[127], alterations in the NHE activity might still compromise the β cell function.

It is widely recognized that blockade of Na/K ATPase by ouabain leads to an increase of intracellular Na^+, thus promoting Ca^{2+} influx – or hampering Ca^{2+} efflux - by the activity of NCX[128]. It has been demonstrated that ouabain is effective even in β cells, where it enhances insulin secretion[118;129]. Moreover, inhibition of NCX activity results in enhancement of insulin secretion, probably because of less

Ca^{2+} extrusion from the cytosol[130]. Since both NHE and NCX are tightly coupled to the Na^+ gradient across the membrane, I_{Na} may be involved directly in pH and Ca_i homeostasis independently from its depolarizing effects on membrane potential.

The VGSC isoforms expressed in pancreatic cells are slightly different between species: whereas Na_V 1.7 seems to be the main isoform in human β cells[103], a fetal brain isoform (putatively $Na_V1.3$) has been found in rats and dogs[131]. In any case, all the VGSC isoforms found in the islets belong to the TTX-sensitive family (IC_{50} in the nanomolar range) and all display both a sizable I_{NaT} and I_{NaL}[132]. More importantly, it has been shown in other cell types that both $Na_V1.7$ and $Na_V1.3$ are sensitive to RAN blockade[55], increasing the possibility that the drug may actually have an impact on the physiological I_{Na} in pancreatic β cells.

Scope of the thesis

Despite the relevant clinical interest about RAN effects on T2DM patients, the impact of I_{NaL} on the pathophysiology of insulin secretion is still unknown. Nevertheless, the complexity of pancreatic islets as integrated systems and the lack of evidences about direct I_{NaL} involvement in the pancreatic β cell physiology are limiting new therapeutic approaches in the treatment of T2DM.

The work in Chapter 2 aims to assess the presence of I_{NaL} and its impact on V_m and Ca_i in a pure population of β cells, represented by the INS-1E β cell line. To evoke spontaneous electrical activity the work used the sulfonylurea tolbutamide instead of glucose, to avoid possible metabolic interferences by the latter. I_{NaL} was investigated by comparing the effects of RAN with those of the common Na^+ channel blocker TTX, in conditions simulating health (tolbutamide only), pharmacological enhancement of I_{NaL} (induced by the alkaloid veratridine) and stressful conditions relevant to T2DM (chronic exposure to high glucose levels).

Reference List of Chapter 1

1. Zaza A, Belardinelli L, Shryock JC. Pathophysiology and pharmacology of the cardiac "late sodium current.". *Pharmacol Ther*. 2008;119:326-339.

2. Zaza A. [The late sodium current: pathophysiology and pharmacology of a new therapeutic target]. *G Ital Cardiol (Rome)*. 2011;12:3S-11S.

3. Zilberter Y, Starmer CF, Starobin J, Grant AO. Late Na channels in cardiac cells: the physiological role of background Na channels. *Biophys J*. 1994;67:153-160.

4. Chaitman BR, Pepine CJ, Parker JO, Skopal J, Chumakova G, Kuch J, Wang W, Skettino SL, Wolff AA. Effects of ranolazine with atenolol, amlodipine, or diltiazem on exercise tolerance and angina frequency in patients with severe chronic angina: a randomized controlled trial. *JAMA*. 2004;291:309-316.

5. Maltsev VA, Silverman N, Sabbah HN, Undrovinas AI. Chronic heart failure slows late sodium current in human and canine ventricular myocytes: implications for repolarization variability. *Eur J Heart Fail*. 2007;9:219-227.

6. Shryock JC, Belardinelli L. Inhibition of late sodium current to reduce electrical and mechanical dysfunction of ischaemic myocardium. *Br J Pharmacol*. 2008;153:1128-1132.

7. Coppini R, Ferrantini C, Yao L, Fan P, Del Lungo M, Stillitano F, Sartiani L, Tosi B, Suffredini S, Tesi C, Yacoub M, Olivotto I, Belardinelli L, Poggesi C, Cerbai E, Mugelli A. Late Sodium Current Inhibition Reverses Electro-Mechanical Dysfunction in Human Hypertrophic Cardiomyopathy. *Circulation*. 2012.

8. Weiss S, Benoist D, White E, Teng W, Saint DA. Riluzole protects against cardiac ischaemia and reperfusion damage via block of the persistent sodium current. *Br J Pharmacol*. 2010;160:1072-1082.

9. Kahlig KM, Lepist I, Leung K, Rajamani S, George AL. Ranolazine selectively blocks persistent current evoked by epilepsy-associated Nanu1.1 mutations. *Br J Pharmacol*. 2010;161:1414-1426.

10. Scirica BM, Morrow DA. Ranolazine in patients with angina and coronary artery disease. *Curr Cardiol Rep*. 2007;9:272-278.

11. Remme CA, Wilde AA. Late Sodium Current Inhibition in Acquired and Inherited Ventricular (dys)function and Arrhythmias. *Cardiovasc Drugs Ther*. 2013.

12. Vatta M, Ackerman MJ, Ye B, Makielski JC, Ughanze EE, Taylor EW, Tester DJ, Balijepalli RC, Foell JD, Li Z, Kamp TJ, Towbin JA. Mutant caveolin-3 induces persistent late sodium current and is associated with long-QT syndrome. *Circulation*. 2006;114:2104-2112.

13. Undrovinas AI, Belardinelli L, Undrovinas NA, Sabbah HN. Ranolazine improves abnormal repolarization and contraction

in left ventricular myocytes of dogs with heart failure by inhibiting late sodium current. *J Cardiovasc Electrophysiol*. 2006;17 Suppl 1:S169-S177.

14. Undrovinas NA, Maltsev VA, Belardinelli L, Sabbah HN, Undrovinas A. Late sodium current contributes to diastolic cell Ca2+ accumulation in chronic heart failure. *J Physiol Sci*. 2010;60:245-257.

15. Sossalla S, Wagner S, Rasenack EC, Ruff H, Weber SL, Schondube FA, Tirilomis T, Tenderich G, Hasenfuss G, Belardinelli L, Maier LS. Ranolazine improves diastolic dysfunction in isolated myocardium from failing human hearts--role of late sodium current and intracellular ion accumulation. *J Mol Cell Cardiol*. 2008;45:32-43.

16. Belardinelli L, Shryock JC, Fraser H. Inhibition of the late sodium current as a potential cardioprotective principle: effects of the late sodium current inhibitor ranolazine. *Heart*. 2006;92 Suppl 4:iv6-iv14.

17. Fraser H, Belardinelli L, Wang L, Light PE, McVeigh JJ, Clanachan AS. Ranolazine decreases diastolic calcium accumulation caused by ATX-II or ischemia in rat hearts. *J Mol Cell Cardiol*. 2006;41:1031-1038.

18. Doshi D, Morrow JP. Potential application of late sodium current blockade in the treatment of heart failure and atrial fibrillation. *Rev Cardiovasc Med*. 2009;10 Suppl 1:S46-S52.

19. Lu YY, Cheng CC, Chen YC, Chen SA, Chen YJ. ATX-II-induced pulmonary vein arrhythmogenesis related to atrial fibrillation and long QT syndrome. *Eur J Clin Invest*. 2012;42:823-831.

20. Hale SL, Shryock JC, Belardinelli L, Sweeney M, Kloner RA. Late sodium current inhibition as a new cardioprotective approach. *J Mol Cell Cardiol*. 2008;44:954-967.

21. Moss AJ, Zareba W, Schwarz KQ, Rosero S, McNitt S, Robinson JL. Ranolazine shortens repolarization in patients

with sustained inward sodium current due to type-3 long-QT syndrome. *J Cardiovasc Electrophysiol*. 2008;19:1289-1293.

22. Wang DW, Yazawa K, George AL, Jr., Bennett PB. Characterization of human cardiac Na+ channel mutations in the congenital long QT syndrome. *Proc Natl Acad Sci U S A*. 1996;93:13200-13205.

23. Burnashev NA, Undrovinas AI, Fleidervish IA, Makielski JC, Rosenshtraukh LV. Modulation of cardiac sodium channel gating by lysophosphatidylcholine. *J Mol Cell Cardiol*. 1991;23 Suppl 1:23-30.

24. Zeng J, Rudy Y. Early afterdepolarizations in cardiac myocytes: mechanism and rate dependence. *Biophys J*. 1995;68:949-964.

25. Burashnikov A, Antzelevitch C. Late-phase 3 EAD. A unique mechanism contributing to initiation of atrial fibrillation. *Pacing Clin Electrophysiol*. 2006;29:290-295.

26. Undrovinas A, Maltsev VA. Late sodium current is a new therapeutic target to improve contractility and rhythm in failing heart. *Cardiovasc Hematol Agents Med Chem*. 2008;6:348-359.

27. Song Y, Shryock JC, Belardinelli L. An increase of late sodium current induces delayed afterdepolarizations and sustained triggered activity in atrial myocytes. *Am J Physiol Heart Circ Physiol*. 2008;294:H2031-H2039.

28. Wu L, Guo D, Li H, Hackett J, Yan GX, Jiao Z, Antzelevitch C, Shryock JC, Belardinelli L. Role of late sodium current in modulating the proarrhythmic and antiarrhythmic effects of quinidine. *Heart Rhythm*. 2008;5:1726-1734.

29. Orth PM, Hesketh JC, Mak CK, Yang Y, Lin S, Beatch GN, Ezrin AM, Fedida D. RSD1235 blocks late INa and suppresses early afterdepolarizations and torsades de pointes induced by class III agents. *Cardiovasc Res*. 2006;70:486-496.

30. Remme CA, Wilde AA. Late Sodium Current Inhibition in Acquired and Inherited Ventricular (dys)function and Arrhythmias. *Cardiovasc Drugs Ther*. 2013;27:91-101.

31. Trenor B, Cardona K, Gomez JF, Rajamani S, Ferrero JM, Jr., Belardinelli L, Saiz J. Simulation and mechanistic investigation of the arrhythmogenic role of the late sodium current in human heart failure. *PLoS One*. 2012;7:e32659.

32. Qian C, Ma J, Zhang P, Luo A, Wang C, Ren Z, Kong L, Zhang S, Wang X, Wu Y. Resveratrol attenuates the na(+)-dependent intracellular ca(2+) overload by inhibiting h(2)o(2)-induced increase in late sodium current in ventricular myocytes. *PLoS One*. 2012;7:e51358.

33. Jiang CM, Han LP, Li HZ, Qu YB, Zhang ZR, Wang R, Xu CQ, Li WM. Calcium-sensing receptors induce apoptosis in cultured neonatal rat ventricular cardiomyocytes during simulated ischemia/reperfusion. *Cell Biol Int*. 2008;32:792-800.

34. Kumar S, Kain V, Sitasawad SL. High glucose-induced Ca2+ overload and oxidative stress contribute to apoptosis of cardiac cells through mitochondrial dependent and independent pathways. *Biochim Biophys Acta*. 2012;1820:907-920.

35. Tamareille S, Achour H, Amirian J, Felli P, Bick RJ, Poindexter B, Geng YJ, Barry WH, Smalling RW. Left ventricular unloading before reperfusion reduces endothelin-1 release and calcium overload in porcine myocardial infarction. *J Thorac Cardiovasc Surg*. 2008;136:343-351.

36. Nakamura TY, Iwata Y, Arai Y, Komamura K, Wakabayashi S. Activation of Na+/H+ exchanger 1 is sufficient to generate Ca2+ signals that induce cardiac hypertrophy and heart failure. *Circ Res*. 2008;103:891-899.

37. Zhong X, Liu J, Lu F, Wang Y, Zhao Y, Dong S, Leng X, Jia J, Ren H, Xu C, Zhang W. Calcium sensing receptor regulates cardiomyocyte function through nuclear calcium. *Cell Biol Int*. 2012;36:937-943.

38. Miller CL, Oikawa M, Cai Y, Wojtovich AP, Nagel DJ, Xu X, Xu H, Florio V, Rybalkin SD, Beavo JA, Chen YF, Li JD, Blaxall BC, Abe J, Yan C. Role of Ca2+/calmodulin-stimulated cyclic nucleotide phosphodiesterase 1 in mediating cardiomyocyte hypertrophy. *Circ Res*. 2009;105:956-964.

39. Lehnart SE, Maier LS, Hasenfuss G. Abnormalities of calcium metabolism and myocardial contractility depression in the failing heart. *Heart Fail Rev*. 2009;14:213-224.

40. Hong CS, Kwon SJ, Cho MC, Kwak YG, Ha KC, Hong B, Li H, Chae SW, Chai OH, Song CH, Li Y, Kim JC, Woo SH, Lee SY, Lee CO, Kim dH. Overexpression of junctate induces cardiac hypertrophy and arrhythmia via altered calcium handling. *J Mol Cell Cardiol*. 2008;44:672-682.

41. Nass RD, Aiba T, Tomaselli GF, Akar FG. Mechanisms of disease: ion channel remodeling in the failing ventricle. *Nat Clin Pract Cardiovasc Med*. 2008;5:196-207.

42. Zheng M, Dilly K, Dos Santos CJ, Li M, Gu Y, Ursitti JA, Chen J, Ross J, Jr., Chien KR, Lederer JW, Wang Y. Sarcoplasmic reticulum calcium defect in Ras-induced hypertrophic cardiomyopathy heart. *Am J Physiol Heart Circ Physiol*. 2004;286:H424-H433.

43. Maltsev VA, Reznikov V, Undrovinas NA, Sabbah HN, Undrovinas A. Modulation of late sodium current by Ca2+, calmodulin, and CaMKII in normal and failing dog cardiomyocytes: similarities and differences. *Am J Physiol Heart Circ Physiol*. 2008;294:H1597-H1608.

44. Wasserstrom JA, Sharma R, O'Toole MJ, Zheng J, Kelly JE, Shryock J, Belardinelli L, Aistrup GL. Ranolazine antagonizes the effects of increased late sodium current on intracellular calcium cycling in rat isolated intact heart. *J Pharmacol Exp Ther*. 2009;331:382-391.

45. Yao L, Fan P, Jiang Z, Viatchenko-Karpinski S, Wu Y, Kornyeyev D, Hirakawa R, Budas GR, Rajamani S, Shryock JC, Belardinelli L. Nav1.5-dependent persistent Na+ influx

activates CaMKII in rat ventricular myocytes and N1325S mice. *Am J Physiol Cell Physiol*. 2011;301:C577-C586.

46. Ma J, Luo A, Wu L, Wan W, Zhang P, Ren Z, Zhang S, Qian C, Shryock JC, Belardinelli L. Calmodulin kinase II and protein kinase C mediate the effect of increased intracellular calcium to augment late sodium current in rabbit ventricular myocytes. *Am J Physiol Cell Physiol*. 2012;302:C1141-C1151.

47. Malloy CR, Buster DC, Castro MM, Geraldes CF, Jeffrey FM, Sherry AD. Influence of global ischemia on intracellular sodium in the perfused rat heart. *Magn Reson Med*. 1990;15:33-44.

48. Dobesh PP, Trujillo TC. Ranolazine: a new option in the management of chronic stable angina. *Pharmacotherapy*. 2007;27:1659-1676.

49. Hasenfuss G, Maier LS. Mechanism of action of the new anti-ischemia drug ranolazine. *Clin Res Cardiol*. 2008;97:222-226.

50. Rajamani S, Shryock JC, Belardinelli L. Rapid kinetic interactions of ranolazine with HERG K+ current. *J Cardiovasc Pharmacol*. 2008;51:581-589.

51. Jia S, Lian J, Guo D, Xue X, Patel C, Yang L, Yuan Z, Ma A, Yan GX. Modulation of the late sodium current by ATX-II and ranolazine affects the reverse use-dependence and proarrhythmic liability of IKr blockade. *Br J Pharmacol*. 2011;164:308-316.

52. Hale SL, Leeka JA, Kloner RA. Improved left ventricular function and reduced necrosis after myocardial ischemia/reperfusion in rabbits treated with ranolazine, an inhibitor of the late sodium channel. *J Pharmacol Exp Ther*. 2006;318:418-423.

53. Chaitman BR, Skettino SL, Parker JO, Hanley P, Meluzin J, Kuch J, Pepine CJ, Wang W, Nelson JJ, Hebert DA, Wolff AA. Anti-ischemic effects and long-term survival during ranolazine monotherapy in patients with chronic severe angina. *J Am Coll Cardiol*. 2004;43:1375-1382.

54. Morrow DA, Scirica BM, Karwatowska-Prokopczuk E, Murphy SA, Budaj A, Varshavsky S, Wolff AA, Skene A, McCabe CH, Braunwald E. Effects of ranolazine on recurrent cardiovascular events in patients with non-ST-elevation acute coronary syndromes: the MERLIN-TIMI 36 randomized trial. *JAMA*. 2007;297:1775-1783.

55. Rajamani S, Shryock JC, Belardinelli L. Block of tetrodotoxin-sensitive, Na(V)1.7 and tetrodotoxin-resistant, Na(V)1.8, Na+ channels by ranolazine. *Channels (Austin)*. 2008;2:449-460.

56. El Bizri N, Kahlig KM, Shyrock JC, George AL, Jr., Belardinelli L, Rajamani S. Ranolazine block of human Na v 1.4 sodium channels and paramyotonia congenita mutants. *Channels (Austin)*. 2011;5:161-172.

57. Djouhri L, Newton R, Levinson SR, Berry CM, Carruthers B, Lawson SN. Sensory and electrophysiological properties of guinea-pig sensory neurones expressing Nav 1.7 (PN1) Na+ channel alpha subunit protein. *J Physiol*. 2003;546:565-576.

58. Chisholm JW, Goldfine AB, Dhalla AK, Braunwald E, Morrow DA, Karwatowska-Prokopczuk E, Belardinelli L. Effect of ranolazine on A1C and glucose levels in hyperglycemic patients with non-ST elevation acute coronary syndrome. *Diabetes Care*. 2010;33:1163-1168.

59. Ning Y, Zhen W, Fu Z, Jiang J, Liu D, Belardinelli L, Dhalla AK. Ranolazine increases beta-cell survival and improves glucose homeostasis in low-dose streptozotocin-induced diabetes in mice. *J Pharmacol Exp Ther*. 2011;337:50-58.

60. Kahn SE. The relative contributions of insulin resistance and beta-cell dysfunction to the pathophysiology of Type 2 diabetes. *Diabetologia*. 2003;46:3-19.

61. Kahn SE. Insulin resistance and beta cell dysfunction: a dual therapeutic approach. *Eur J Clin Invest*. 2002;32 Suppl 3:1-2.

62. Shaw JE, Sicree RA, Zimmet PZ. Global estimates of the prevalence of diabetes for 2010 and 2030. *Diabetes Res Clin Pract*. 2010;87:4-14.

63. Diagnosis and classification of diabetes mellitus. *Diabetes Care*. 2008;31 Suppl 1:S55-S60.

64. Lin Y, Sun Z. Current views on type 2 diabetes. *J Endocrinol*. 2010;204:1-11.

65. Costes S, Langen R, Gurlo T, Matveyenko AV, Butler PC. beta-Cell Failure in Type 2 Diabetes: A Case of Asking Too Much of Too Few? *Diabetes*. 2013;62:327-335.

66. Rhodes CJ. Type 2 diabetes-a matter of beta-cell life and death? *Science*. 2005;307:380-384.

67. Cifarelli V, Geng X, Styche A, Lakomy R, Trucco M, Luppi P. C-peptide reduces high-glucose-induced apoptosis of endothelial cells and decreases NAD(P)H-oxidase reactive oxygen species generation in human aortic endothelial cells. *Diabetologia*. 2011;54:2702-2712.

68. Luppi P, Cifarelli V, Tse H, Piganelli J, Trucco M. Human C-peptide antagonises high glucose-induced endothelial

dysfunction through the nuclear factor-kappaB pathway. *Diabetologia*. 2008;51:1534-1543.

69. Luppi P, Cifarelli V, Wahren J. C-peptide and long-term complications of diabetes. *Pediatr Diabetes*. 2011;12:276-292.

70. Best L, Brown PD, Sener A, Malaisse WJ. Electrical activity in pancreatic islet cells: The VRAC hypothesis. *Islets*. 2010;2:59-64.

71. Best L, Brown PD. Studies of the mechanism of activation of the volume-regulated anion channel in rat pancreatic beta-cells. *J Membr Biol*. 2009;230:83-91.

72. Straub SG, James RF, Dunne MJ, Sharp GW. Glucose activates both K(ATP) channel-dependent and K(ATP) channel-independent signaling pathways in human islets. *Diabetes*. 1998;47:758-763.

73. Orecna M, Hafko R, Bacova Z, Podskocova J, Chorvat D, Jr., Strbak V. Different secretory response of pancreatic islets and

insulin secreting cell lines INS-1 and INS-1E to osmotic stimuli. *Physiol Res*. 2008;57:935-945.

74. Gustavsson N, Wei SH, Hoang DN, Lao Y, Zhang Q, Radda GK, Rorsman P, Sudhof TC, Han W. Synaptotagmin-7 is a principal Ca2+ sensor for Ca2+ -induced glucagon exocytosis in pancreas. *J Physiol*. 2009;587:1169-1178.

75. Rorsman P, Braun M. Regulation of Insulin Secretion in Human Pancreatic Islets. *Annu Rev Physiol*. 2012.

76. Saadeh M, Ferrante TC, Kane A, Shirihai O, Corkey BE, Deeney JT. Reactive oxygen species stimulate insulin secretion in rat pancreatic islets: studies using mono-oleoyl-glycerol. *PLoS One*. 2012;7:e30200.

77. Nolan CJ, Madiraju MS, Delghingaro-Augusto V, Peyot ML, Prentki M. Fatty acid signaling in the beta-cell and insulin secretion. *Diabetes*. 2006;55 Suppl 2:S16-S23.

78. Roduit R, Nolan C, Alarcon C, Moore P, Barbeau A, Delghingaro-Augusto V, Przybykowski E, Morin J, Masse F, Massie B, Ruderman N, Rhodes C, Poitout V, Prentki M. A role for the malonyl-CoA/long-chain acyl-CoA pathway of lipid signaling in the regulation of insulin secretion in response to both fuel and nonfuel stimuli. *Diabetes*. 2004;53:1007-1019.

79. Eliasson L, Renstrom E, Ding WG, Proks P, Rorsman P. Rapid ATP-dependent priming of secretory granules precedes Ca(2+)-induced exocytosis in mouse pancreatic B-cells. *J Physiol*. 1997;503 (Pt 2):399-412.

80. Kitaguchi T, Oya M, Wada Y, Tsuboi T, Miyawaki A. Extracellular Calcium influx activates Adenylate Cyclase 1 and potentiates Insulin secretion in MIN6 cells. *Biochem J*. 2013.

81. Zawalich WS, Bonnet-Eymard M, Zawalich KC. Signal transduction in pancreatic beta-cells: regulation of insulin secretion by information flow in the phospholipase C/protein kinase C pathway. *Front Biosci*. 1997;2:d160-d172.

82. Renstrom E, Eliasson L, Rorsman P. Protein kinase A-dependent and -independent stimulation of exocytosis by cAMP in mouse pancreatic B-cells. *J Physiol*. 1997;502 (Pt 1):105-118.

83. Sone H, Ito M, Sugiyama K, Ohneda M, Maebashi M, Furukawa Y. Biotin enhances glucose-stimulated insulin secretion in the isolated perfused pancreas of the rat. *J Nutr Biochem*. 1999;10:237-243.

84. Haber EP, Procopio J, Carvalho CR, Carpinelli AR, Newsholme P, Curi R. New insights into fatty acid modulation of pancreatic beta-cell function. *Int Rev Cytol*. 2006;248:1-41.

85. Di Cairano ES, Davalli AM, Perego L, Sala S, Sacchi VF, La Rosa S, Finzi G, Placidi C, Capella C, Conti P, Centonze VE, Casiraghi F, Bertuzzi F, Folli F, Perego C. The glial glutamate transporter 1 (GLT1) is expressed by pancreatic beta-cells and prevents glutamate-induced beta-cell death. *J Biol Chem*. 2011;286:14007-14018.

86. Gromada J, Holst JJ, Rorsman P. Cellular regulation of islet hormone secretion by the incretin hormone glucagon-like peptide 1. *Pflugers Arch*. 1998;435:583-594.

87. Strowski MZ, Kohler M, Chen HY, Trumbauer ME, Li Z, Szalkowski D, Gopal-Truter S, Fisher JK, Schaeffer JM, Blake AD, Zhang BB, Wilkinson HA. Somatostatin receptor subtype 5 regulates insulin secretion and glucose homeostasis. *Mol Endocrinol*. 2003;17:93-106.

88. Dunbar JC, Walsh MF. Glucagon and insulin secretion by dispersed islet cells: possible paracrine relationships. *Horm Res*. 1982;16:257-267.

89. Kanno T, Gopel SO, Rorsman P, Wakui M. Cellular function in multicellular system for hormone-secretion: electrophysiological aspect of studies on alpha-, beta- and delta-cells of the pancreatic islet. *Neurosci Res*. 2002;42:79-90.

90. Schusdziarra V, Schmid R. Physiological and pathophysiological aspects of somatostatin. *Scand J Gastroenterol Suppl*. 1986;119:29-41.

91. Braun M, Ramracheya R, Rorsman P. Autocrine regulation of insulin secretion. *Diabetes Obes Metab*. 2012;14 Suppl 3:143-151.

92. Gros L, Virsolvy A, Salazar G, Bataille D, Blache P. Characterization of low-affinity binding sites for glibenclamide on the Kir6.2 subunit of the beta-cell KATP channel. *Biochem Biophys Res Commun*. 1999;257:766-770.

93. Lawrence CL, Proks P, Rodrigo GC, Jones P, Hayabuchi Y, Standen NB, Ashcroft FM. Gliclazide produces high-affinity block of KATP channels in mouse isolated pancreatic beta cells but not rat heart or arterial smooth muscle cells. *Diabetologia*. 2001;44:1019-1025.

94. Roe MW, Worley JF, III, Mittal AA, Kuznetsov A, DasGupta S, Mertz RJ, Witherspoon SM, III, Blair N, Lancaster ME,

McIntyre MS, Shehee WR, Dukes ID, Philipson LH. Expression and function of pancreatic beta-cell delayed rectifier K+ channels. Role in stimulus-secretion coupling. *J Biol Chem*. 1996;271:32241-32246.

95. Finol-Urdaneta RK, Remedi MS, Raasch W, Becker S, Clark RB, Struver N, Pavlov E, Nichols CG, French RJ, Terlau H. Block of Kv1.7 potassium currents increases glucose-stimulated insulin secretion. *EMBO Mol Med*. 2012;4:424-434.

96. Jacobson DA, Kuznetsov A, Lopez JP, Kash S, Ammala CE, Philipson LH. Kv2.1 ablation alters glucose-induced islet electrical activity, enhancing insulin secretion. *Cell Metab*. 2007;6:229-235.

97. Monge L, Silvestre RA, Miralles P, Peiro E, Villanueva ML, Marco J. In vitro effects of BAY K 8644, a dihydropyridine derivative with hypoglycaemic properties, on hepatic glucose production and pancreatic hormone secretion. *Biochem Pharmacol*. 1988;37:2933-2937.

98. Panten U, Zielmann S, Schrader MT, Lenzen S. The dihydropyridine derivative, Bay K 8644, enhances insulin secretion by isolated pancreatic islets. *Naunyn Schmiedebergs Arch Pharmacol*. 1985;328:351-353.

99. Lebrun P, Arkhammar P, Antoine MH, Nguyen QA, Hansen JB, Pirotte B. A potent diazoxide analogue activating ATP-sensitive K+ channels and inhibiting insulin release. *Diabetologia*. 2000;43:723-732.

100. Liu G, Hilliard N, Hockerman GH. Cav1.3 is preferentially coupled to glucose-induced [Ca2+]i oscillations in the pancreatic beta cell line INS-1. *Mol Pharmacol*. 2004;65:1269-1277.

101. Taylor JT, Huang L, Keyser BM, Zhuang H, Clarkson CW, Li M. Role of high-voltage-activated calcium channels in glucose-regulated beta-cell calcium homeostasis and insulin release. *Am J Physiol Endocrinol Metab*. 2005;289:E900-E908.

102. Al Mahmood HA, el Khatim MS, Gumaa KA, Thulesius O. The effect of calcium-blockers nicardipine, darodipine, PN-200-110 and nifedipine on insulin release from isolated rat pancreatic islets. *Acta Physiol Scand*. 1986;126:295-298.

103. Braun M, Ramracheya R, Bengtsson M, Zhang Q, Karanauskaite J, Partridge C, Johnson PR, Rorsman P. Voltage-gated ion channels in human pancreatic beta-cells: electrophysiological characterization and role in insulin secretion. *Diabetes*. 2008;57:1618-1628.

104. Miller C. An overview of the potassium channel family. *Genome Biol*. 2000;1:REVIEWS0004.

105. Ashcroft FM, Gribble FM. Correlating structure and function in ATP-sensitive K+ channels. *Trends Neurosci*. 1998;21:288-294.

106. Stephan D, Winkler M, Kuhner P, Russ U, Quast U. Selectivity of repaglinide and glibenclamide for the pancreatic

over the cardiovascular K(ATP) channels. *Diabetologia*. 2006;49:2039-2048.

107. Korytkowski MT. Sulfonylurea treatment of type 2 diabetes mellitus: focus on glimepiride. *Pharmacotherapy*. 2004;24:606-620.

108. Rendell M. The role of sulphonylureas in the management of type 2 diabetes mellitus. *Drugs*. 2004;64:1339-1358.

109. Hatlapatka K, Willenborg M, Rustenbeck I. Plasma membrane depolarization as a determinant of the first phase of insulin secretion. *Am J Physiol Endocrinol Metab*. 2009;297:E315-E322.

110. Rosati B, Marchetti P, Crociani O, Lecchi M, Lupi R, Arcangeli A, Olivotto M, Wanke E. Glucose- and arginine-induced insulin secretion by human pancreatic beta-cells: the role of HERG K(+) channels in firing and release. *FASEB J*. 2000;14:2601-2610.

111. Goforth PB, Bertram R, Khan FA, Zhang M, Sherman A, Satin LS. Calcium-activated K+ channels of mouse beta-cells are controlled by both store and cytoplasmic Ca2+: experimental and theoretical studies. *J Gen Physiol*. 2002;120:307-322.

112. Dai XQ, Manning Fox JE, Chikvashvili D, Casimir M, Plummer G, Hajmrle C, Spigelman AF, Kin T, Singer-Lahat D, Kang Y, Shapiro AM, Gaisano HY, Lotan I, MacDonald PE. The voltage-dependent potassium channel subunit Kv2.1 regulates insulin secretion from rodent and human islets independently of its electrical function. *Diabetologia*. 2012;55:1709-1720.

113. Mears D, Rojas E. Properties of voltage-gated Ca2+ currents measured from mouse pancreatic beta-cells in situ. *Biol Res*. 2006;39:505-520.

114. Vignali S, Leiss V, Karl R, Hofmann F, Welling A. Characterization of voltage-dependent sodium and calcium channels in mouse pancreatic A- and B-cells. *J Physiol*. 2006;572:691-706.

115. Johnson JD, Kuang S, Misler S, Polonsky KS. Ryanodine receptors in human pancreatic beta cells: localization and effects on insulin secretion. *FASEB J*. 2004;18:878-880.

116. Dean PM, Matthews EK. Electrical activity in pancreatic islet cells: effect of ions. *J Physiol*. 1970;210:265-275.

117. Meissner HP, Schmelz H. Membrane potential of beta-cells in pancreatic islets. *Pflugers Arch*. 1974;351:195-206.

118. Donatsch P, Lowe DA, Richardson BP, Taylor P. The functional significance of sodium channels in pancreatic beta-cell membranes. *J Physiol*. 1977;267:357-376.

119. Wahl MA, Anulukanapakorn K, Ammon HP. Effect of a sodium-channel activator (BDF 9148) on insulin secretion in mouse pancreatic islets. *Naunyn Schmiedebergs Arch Pharmacol*. 1997;355:417-421.

120. Ernst SJ, Aguilar-Bryan L, Noebels JL. Sodium channel beta1 regulatory subunit deficiency reduces pancreatic islet glucose-

stimulated insulin and glucagon secretion. *Endocrinology*. 2009;150:1132-1139.

121. Hiriart M, Matteson DR. Na channels and two types of Ca channels in rat pancreatic B cells identified with the reverse hemolytic plaque assay. *J Gen Physiol*. 1988;91:617-639.

122. Barnett DW, Pressel DM, Misler S. Voltage-dependent Na+ and Ca2+ currents in human pancreatic islet beta-cells: evidence for roles in the generation of action potentials and insulin secretion. *Pflugers Arch*. 1995;431:272-282.

123. Pressel DM, Misler S. Role of voltage-dependent ionic currents in coupling glucose stimulation to insulin secretion in canine pancreatic islet B-cells. *J Membr Biol*. 1991;124:239-253.

124. Plant TD. Na+ currents in cultured mouse pancreatic B-cells. *Pflugers Arch*. 1988;411:429-435.

125. Lou XL, Yu X, Chen XK, Duan KL, He LM, Qu AL, Xu T, Zhou Z. Na+ channel inactivation: a comparative study between pancreatic islet beta-cells and adrenal chromaffin cells in rat. *J Physiol*. 2003;548:191-202.

126. Stiernet P, Nenquin M, Moulin P, Jonas JC, Henquin JC. Glucose-induced cytosolic pH changes in beta-cells and insulin secretion are not causally related: studies in islets lacking the Na+/H+ exchangeR NHE1. *J Biol Chem*. 2007;282:24538-24546.

127. Lehninger A. Principles of Biochemistry. 1982.

128. McDonough AA, Velotta JB, Schwinger RH, Philipson KD, Farley RA. The cardiac sodium pump: structure and function. *Basic Res Cardiol*. 2002;97 Suppl 1:I19-I24.

129. Kajikawa M, Fujimoto S, Tsuura Y, Mukai E, Takeda T, Hamamoto Y, Takehiro M, Fujita J, Yamada Y, Seino Y. Ouabain suppresses glucose-induced mitochondrial ATP

production and insulin release by generating reactive oxygen species in pancreatic islets. *Diabetes*. 2002;51:2522-2529.

130. Hamming KS, Soliman D, Webster NJ, Searle GJ, Matemisz LC, Liknes DA, Dai XQ, Pulinilkunnil T, Riedel MJ, Dyck JR, MacDonald PE, Light PE. Inhibition of beta-cell sodium-calcium exchange enhances glucose-dependent elevations in cytoplasmic calcium and insulin secretion. *Diabetes*. 2010;59:1686-1693.

131. Philipson LH, Kusnetsov A, Larson T, Zeng Y, Westermark G. Human, rodent, and canine pancreatic beta-cells express a sodium channel alpha 1-subunit related to a fetal brain isoform. *Diabetes*. 1993;42:1372-1377.

132. Catterall WA, Goldin AL, Waxman SG. International Union of Pharmacology. XXXIX. Compendium of voltage-gated ion channels: sodium channels. *Pharmacol Rev*. 2003;55:575-578.

CHAPTER 2 – THE LATE SODIUM CURRENT (I_{NaL}) IN PANCREATIC β CELLS: FUNCTIONAL CHARACTERIZATION AND ROLE IN INSULIN SECRETION

Rizzetto R., Rocchetti M., Villa A., Sala L., Ronchi C., Bertuzzi F., Belardinelli L. and Zaza A.

Under submission

Abstract

AIM: To characterize the late sodium current (I_{NaL}) in a pure pancreatic β-cell population and its impact on the membrane potential (V_m), intracellular Ca^{2+} (Ca_i) and glucose-stimulated insulin secretion (GSIS).

METHODS: I_{Na} was blocked by 10 μM ranolazine (RAN) or 0.5 μM tetrodotoxin (TTX) and identified as the respective subtraction currents (I_{RAN} and I_{TTX}); veratridine (VERA) was used as I_{NaL} enhancer. The effects of I_{NaL} modulation on tolbutamide (TOLB) or glucose-induced electrical activity were assessed by patch clamp. Slow V-ramps (0.056 V/s) were used to isolate the steady-state activated currents. Ca_i changes elicited by step depolarizations were optically measured in Fluo4AM-loaded cells. GSIS was measured from cell supernatants by HTRF assay (Cisbio). **RESULTS:** TOLB-induced action potential firing was abolished by TTX but not by RAN. I_{NaL} enhancement by VERA resulted in strong depolarization, an effect counteracted by both RAN and TTX. Under baseline I_{TTX} and I_{RAN} were similar, with minor differences in threshold. Both I_{TTX} and

I_{RAN} had a reversal potentials (E_{rev}) negative to that expected from pure I_{Na} (E_{Na}). VERA strongly increased I_{TTX} and, to a much lesser extent, I_{RAN}. K^+ -channels blockade shifted E_{rev} of I_{RAN} and I_{TTX} toward E_{Na} , thus revealing coupling of I_{NaL} to a Na-activated K^+ conductance (I_{KNa}). Selective I_{KNa} activation by bithionol (10 μM, in the presence of VERA) strongly hyperpolarized V_m and negatively shifted the E_{rev} of I_{TTX}. Transcript analysis (RT-PCR) detected the expression of *Slick* and *Slack* channels, known to underlie I_{KNa}. I_{NaL} blockade (by TTX) reduced Ca_i response to V steps (-10, 0 and +20 mV), with maximal effect at 0 mV. Ca_i decay was accelerated by TTX, as expected from enhancement of Na^+ /Ca^{2+} exchange. Chronic (24-72 hrs) exposure of INS-1E cells to 33 mM glucose markedly increased inward I_{TTX} and I_{RAN}, to indicate I_{NaL} enhancement by hyperglycemic stress (HG). Under baseline TTX and RAN did not affect GSIS; VERA strongly enhanced GSIS, an effect reversed by TTX and RAN. GSIS was strongly blunted by chronic I_{NaL} enhancement (HG or VERA) and partially restored by concomitant exposure to RAN.

CONCLUSIONS: I_{NaL} is significantly expressed in pancreatic β cells and is functionally coupled to I_{KNa}; by limiting I_{NaL}-induced depolarization, the latter might amplify Na^+ influx and thus Ca_i overload. I_{NaL} blockade by RAN may decrease GSIS acutely, but it may improve GSIS when I_{NaL} is chronically enhanced by HG. These observations suggest I_{NaL} involvement in insulin deficiency and may provide a mechanistic interpretation of the positive effects of ranolazine on glycemic control in patients.

Introduction

Stimulus-secretion coupling in pancreatic β cells is a key factor modulating insulin secretion. Under normal conditions the response of β cells to an increase of plasma glucose levels is a biphasic phenomenon. Whereas the second phase is largely metabolic and involves complex intracellular pathways [1;2], the first phase of insulin secretion is dependent on membrane electrical activity. It is widely accepted that in β-cells an acute exposure to high glucose leads to K_{ATP} channels closure, thus leading to Ca^{2+} entry into the cell following membrane depolarization. It has been shown that the membrane depolarization caused by K_{ATP} closure triggers spontaneous action potentials, driven by voltage-gated Na^{+} and Ca^{2+} channels[3;4], which in turn open voltage-gated K^{+} channels that provide repolarization necessary for continuous action potential (AP) firing. Thus, the first phase of glucose-stimulated insulin secretion (GSIS) depends on the functional interplay between depolarizing (Na^{+} and Ca^{2+}) and hyperpolarizing (K^{+}) currents.[3]

Recent works have highlighted the beneficial effects of ranolazine (RAN), an antianginal drug, on plasma glucose levels and glycosylated hemoglobin (HbA1c) in type II diabetic patients.[5] Moreover, RAN was found able to improve glucose homeostasis in diabetic mice by directly increasing insulin secretion from pancreatic islets, because of prevention of β cell loss[6]. However, the molecular mechanisms of these evidences remain still unclear.

Since the pancreatic islet works as an integrated system in which β cell activity is tightly coupled with other cell types (*i.e.* the glucagon-producing α cells), the direct effect of RAN on β cells is

still debated. Furthermore, albeit RAN is a well known blocker of the late sodium current (I_{NaL}), the direct involvement of I_{NaL} in β-cells electrical activity and function is still unknown.

In cardiac myocytes I_{NaL} is enhanced by reactive oxygen species (ROS)[7] and hypoxia[8;9] all conditions known to be present in β cell dysfunction[10-12]. The existing evidence on Na^+ channel activity in pancreatic islets is restricted to the transient I_{Na}[3;4;13;14] and the novel effects of RAN provide the rationale to investigate the relevancy of I_{NaL} and its enhancement on the single β cell function.

The aim of this work was to characterize I_{NaL} in a pure population of pancreatic β-cells, represented by the INS-1E cell line, under stimulated conditions. To isolate I_{NaL} univocally, we compared the effect of RAN on steady-state activated currents with the common Na^+ channel blocker TTX. To avoid metabolic disturbances by glucose we used the sulfonylurea tolbutamide (TOLB) to provide K_{ATP} closure and AP firing. Since pathophysiological enhancement of I_{NaL} is a major cause of damage in the heart[15-17], we used the Na^+ channel opener veratridine and a model of chronic hyperglycemia to test the hypothesis that an abnormal increase of I_{NaL} may be involved in functional derangements of pancreatic β cells.

Methods

Cell culture and maintainance

INS-1E cell line, a kind gift of Dr. Wollheim (University of Geneve, Switzerland), were cultured in RPMI medium (Sigma) supplemented with 10% FBS, 2 mM L-glutamine, 1 mM Na-pyruvate, 50 μM 2-mercaptoethanol and 10 mM glucose.

For chronic exposure to high glucose (HG) experiments, cells were plated in medium Petri dishes at a density of 90000 cells/dish and left in glucose-free medium overnight. Cells were washed once with PBS and put in complete medium with 33 mM glucose for 24 hours. The day of experiment cells were washed twice with complete medium with 2.5 mM glucose and left in 2.5 mM glucose Krebs for the measurement.

Electrophysiology

For electrophysiology measurements, cells were disattached the day before and plated in 35mm Petri dishes at a density of 100000 cells/dish. All data was acquired by a MultiClamp 700A amplifier (Axon Instruments) at 5 kHz (2 kHz for V-Clamp measurements), filtered at 1 kHz (Axon Digidata 1200) and analyzed with a dedicated software (pCLAMP 9.0).

I-Clamp

Current clamp experiments were carried out at 35°C in the perforated patch configuration. All measurements were started when the access resistance was stable and lower than 20 MΩ. Changes in V_m were recorded by gap-free protocols in which test substances were superimposed. All experiments were performed in the presence of 2.5 mM glucose and 50 μM TOLB (Sigma).

V-Clamp

The ruptured patch configuration was used to identify TTX- and RAN- sensitive currents (I_{TTX} and I_{RAN}, respectively) activated during slow voltage ramps (0.056 V/s over 2.5 s, one pulse every 6 s) in the presence of test substances. All experiments were performed using 50 μM TOLB as baseline and in 2.5 mM glucose conditions.

Intracellular Ca^{2+} measurements

INS-1E cells were plated on fluorodishes at a density of 150000 cells/dish two days before the measurement. Cells were incubated with 10 μM Fluo4-AM for 45 min followed by 15 min washout, then put on an inverted microscope. Ca^{2+} increments were evoked by step depolarizations from -80 mV to the test potentials (-10, 0, 20 mV) in the perforated patch configuration. All experiments were performed at 35°C in 2.5 mM glucose and 50 μM TOLB was present in the extracellular solution. Ca^{2+} decrements at the end of the step were fitted by a monoexponential equation to obtain the time constant (τ) of decay.

Solutions

Standard extracellular solution (Krebs) contained (in mM) 140 NaCl, 3.6 KCl, 2 $NaHCO_3$, 0.5 NaH_2PO_4, 0.5 $MgSO_4$, 5 HEPES, 1.5 $CaCl_2$, 2.5 glucose (pH 7.4).

For perforated patch, intracellular solution contained (in mM) 76 K_2SO_4, 10 NaCl, 10 KCl, 1 $MgCl_2$, 5 HEPES (pH 7.35). Freshly prepared amphotericin B (Sigma) was added before the experiment to reach a final concentration of 0.3 mM.

For ruptured patch, intracellular solution contained (in mM) 95 K-gluconate, 30 KCl, 1 $MgCl_2$, 5 HEPES, 5 Na_2ATP, 1 Na_2GTP, 1 EGTA, 0.4 $CaCl_2$, (pH 7.2).

50 μM TOLB was present in Krebs solution for all experiments. For some measurements 40 μM veratridine (Alomone Labs, Israel) and 10 μM bithionol (Sigma) were added to the standard Krebs.

For K-blockade experiments (K-blockade Krebs, KBK), 10 mM TEA-chloride and 0.5 mM 4 aminopyridine (Sigma) were added to the standard Krebs, without removing NaCl in order to keep the Na^+ gradient across the membrane.

TTX (Tocris, UK) was dissolved in water, ranolazine (Gilead Sciences, California) was dissolved in 0.1 M HCl and they were included in the Krebs solution at the concentration indicated. TOLB, bithionol were dissolved in DMSO. DMSO was balanced in all test solutions, in all conditions it never surpassed 1%.

Real time qPCR

Relative expression of mRNAs encoding Slo 2.1, Slo 2.2 and the NaV isoforms, was measured by RTq-PCR as previously described. Briefly, total RNA was extracted from INS1-E cells and its concentration and purity was determined as the 260/280 nm ratio (NanoDrop Thermo Scientific). One microgram of each RNA sample was reverse transcribed to cDNA using the 5X iScript cDNA Synthesis Kit system (Bio-Rad Laboratories, Hercules, United States). The amplification reaction was performed with SSoFast EvaGreen (Bio-Rad Laboratories, Hercules, United States) and specific primers (Table 1) designed using NCBI Primer3-Blast[18].

Signal detection and analyses of results were performed using ABI Prism 7500 Sequence Detection System software (v1.6). Relative quantification was achieved with the comparative ΔΔCt method[19] by normalization for β-Actin or GAPDH (data not shown). All samples were amplified in triplicate from the same RNA preparation and the mean value was computed.

Insulin secretion

For glucose-stimulated insulin secretion (GSIS) measurements, INS-1E cells were plated in 96-multiwell dishes at a density of 10000 cells/well and cultured in normal medium. Two days after plating, cells were washed once with glucose-free Krebs supplemented with 0.1% BSA and incubated in 2.5 mM glucose Krebs (0.1% BSA) for 45 minutes. After this pre-incubation, cells were washed once with glucose-free Krebs (0.1% BSA) and incubated for 1 hour in Krebs (0.1% BSA) supplemented with test substances. Supernatants were then collected for insulin measurements.

For chronic treatment, the cells were plated at the same density in the multiwell. After the first day medium was substituted with complete medium supplemented with 10 mM glucose (controls), 33 mM glucose (HG group), 33 mM glucose +10 mM ranolazine (HG+RAN group) or 40 mM veratridine (VERA group). Medium was changed every day to prevent drug degradation. After 72 h cells were washed twice with glucose-free Krebs (0.1% BSA) and then the glucose-challenge test was performed. Insulin was detected from the supernatants and measured with a HTRF assay (Cisbio). Test substances were dissolved in the same solvents used for

electrophysiology. DMSO was balanced in each well, in any condition it never surpassed 1%.

Statistical analysis

All data was analyzed using paired or unpaired t-test, as requested. For multiple comparisons we used one-way ANOVA with Tukey or Bonferroni correction, depending on the experimental conditions.

Results

I_{NaL} impact on tolbutamide-induced electrical activity

To assess the effect of I_{NaL} blockers on V_m under stimulated conditions, we used 50 μM TOLB to induce spontaneous firing of action potentials (AP). V_m was monitored by gap-free recordings in the perforated patch configuration. The effect of I_{NaL} blockade was studied under baseline conditions and in the presence of I_{NaL} enhancement by veratridine (40 μM, VERA).

Baseline: Whereas 0.5 μM TTX abolished AP firing almost completely, 10 μM RAN didn't prevent AP upstroke (Fig. 1A and 1B, respectively) and slightly depolarized the minimum interspike potential (TOLB: -35.6±2 mV; RAN: -28.9±2 mV; $p<0.05$).

VERA: As shown in fig.2, VERA markedly depolarized V_m (to -6.2±3.8 m; $p<0.005$ vs baseline) and completely stopped spontaneous AP firing. In the presence of VERA, both TTX and RAN hyperpolarized V_m, with TTX being more potent than RAN (TTX: -24.4±2.7 mV; $p<0.05$ vs VERA. RAN: -16.2±4 mV; $p<0.05$ vs VERA).

Steady-state I_{TTX} and I_{RAN}

TTX- and RAN-sensitive currents (I_{TTX} and I_{RAN} respectively) were isolated as subtraction currents. To avoid subtraction artefacts caused by time-varying I_{KATP} activation, the latter current was blocked by including 50 μM TOLB in the extracellular solution and 5 mM ATP in the intracellular one. The I/V relationships of steady-state I_{TTX} and I_{RAN} were obtained by applying slow depolarizing ramps (0.056 V/s over 2 s from a holding of -100 mV) under ruptured patch configuration.

As shown in fig. 3, although mean inward current density was similar (TTX: -3.29±0.46 pA/pF; RAN: -3.4 ±0.5 pA/pF; N.S.), the activation threshold (E_{TH})was significantly more negative for I_{TTX} than for I_{RAN} (TTX: -26±2 mV, RAN: -17.9± 2.8 mV; $p< 0.05$). I_{TTX} recorded in β cells from human pancreatic islets had similar I/V relationship. (Suppl. Fig. 4). Both I_{RAN} and I_{TTX} included a marked outward component and their reversal potential (E_{REV}, TTX: 11.3±3.5 mV; RAN: 15.4±2.1 mV; N.S.) was substantially negative to that expected for a pure Na^+ conductance under this experimental conditions (E_{Na}: 64 mV). This indicates the presence of an outward conductance inhibited by both agents; the high TTX selectivity for Na^+ channels implies that such conductance is activated by Na^+ influx. RT-PCR analysis confirmed the presence of several isoforms of the Na^+ channel (Fig 3C), classically defined as 'neuronal' subtypes[20]. The main isoform was Na_V 1.3, whose levels were quantitatively comparable with K_{IR} 6.2 (K_{ATP} channel) mRNA.

I_{TTX} and I_{RAN} modulation by veratridine

As shown in fig. 4, VERA strongly affected I_{TTX}. It shifted I_{TTX} activation threshold by about -24 mV (CTRL: -26.7±2 mV; VERA: -49.7±3 mV; $p<0.05$); increased mean inward current twofold (CTRL: -3.29±0.46 pA/pF; VERA: -6.17±0.65 pA/pF; $p<0.05$) and moved E_{rev} by +20 mV, *i.e.* to approach the predicted E_{Na} (CTRL: 11.2±3.54 mV; VERA: 31.6±4.09 mV; $p<0.01$). The substantial negative shift in E_{TH} points to enhancement of I_{NaL} through a set of TTX-S channels. The large shift in E_{rev} suggests that, under VERA, I_{NaL} becomes largely predominant in the balance between I_{NaL} and the Na^+ -activated outward component.

VERA effect on I_{RAN} was much smaller, mean inward density remaining unchanged (CTRL: -3.41±0.5 pA/pF; VERA: -5.37±0.6 pA/pF; N.S.). This was mainly because the negative E_{TH} shift was limited to -10 mV (CTRL: -17.9±2.8 mV; VERA: -28.06±2.1 mV; $p<0.05$) and E_{REV} was not significantly affected (CTRL: 15.4±2.1 mV; VERA: 13.1±4.1 mV; N.S.). Failure of E_{rev} to change suggests that in the case of I_{RAN} the balance between I_{NaL} and the Na^+ -activated outward component was substantially preserved even in the presence of VERA.

The effects of VERA on E_{TH} of I_{TTX} is consistent with previous reports [21]. The differences between I_{TTX} and I_{RAN} in response to VERA suggest 1) VERA enhancement of a set of low-threshold Na^+ channels, which are TTX-sensitive, but not RAN-sensitive; 2) weak coupling of RAN-insensitive channels to activation of the Na^+-activated outward component.

Nature of the outward component of I_{TTX} and I_{RAN}

K^+ currents are strongly represented in the global steady-state I/V relationship of INS-1E (Suppl. Fig. 1) and obvious candidates to account for the outward component contributing to I_{TTX} and I_{RAN}. Therefore, I_{TTX} and I_{RAN} were evaluated in the presence of conditions blocking a wide spectrum of K^+ channels (KBK solution, described in methods). As shown in fig. 5, KBK abolished the outward component of both I_{TTX} and I_{RAN} similarly and this was associated with a shift of E_{REV} towards the theoretical E_{Na} (TTX, CTRL: 11.28±3.53 mV, KBK: 39.2±5.1 mV; $p<0.01$ RAN, CTRL: 15.4±2 mV, KBK: 31.87±4.4 mV; $p<0.01$). KBK was expected to unveil Na^+ contribution to I_{TTX} and I_{RAN}; in spite of this, the inward peak amplitude was slightly

reduced by KBK, thus suggesting ancillary Na^+ channel blockade by KBK components. Furthermore, in the presence of KBK the activation threshold of I_{TTX} became identical to that of I_{RAN}, which was significantly more positive under control conditions.

Sensitivity to KBK indicates that the outward components of I_{TTX} and I_{RAN} are supported by K^+ channels. Whereas both RAN and TTX are Na^+ channel blockers, ancillary blockade of a K^+ current (I_{ERG}) is a known property of RAN only[22]; therefore, the K^+ component shared by I_{TTX} and I_{RAN} must be linked to Na^+ influx and likely represented by I_{KNa}. Furthermore, the I/V relationship of total membrane current, measured in the same conditions under which I_{TTX} and I_{RAN} were evaluated, was unaffected by E4031 (5μM), thus indicating negligible I_{ERG} contribution (online supplement).

I_{KNa} molecular identity and functional contribution

The putative molecular identity of I_{KNa} is represented by Na^+-activated K^+ channels (KNaC). Therefore, the expression of KNaC gene transcripts (*Slick* and *Slack*) was assessed by quantitative RT-PCR on INS-1E cell lysates. Both *Slick* and *Slack* transcripts were clearly detected and their expression level was similar(Fig. 5C)

While I_{KNa} is blocked by KBK components [23;24], selective blockers are not available for this current. Therefore, I_{KNa} functional expression was evaluated by enhancing it with the specific *Slack* channel activator bithionol (10 μM)[25]. The effect of bithionol on V_m and I_{TTX} was tested in the presence of 40 μM VERA, to simulate the condition of I_{NaL} enhancement. As shown in Fig 6A, bithionol hyperpolarized V_m to a value(-40.2±3.02 mV) similar to I_{TTX} activation threshold (light trace in Fig 4A). I_{TTX} I/V relationship

(recorded in the presence of VERA) was modified by bithionol in a way compatible to the activation of a large K^+ conductance. In spite of its remarkable impact on the I/V contour, bithionol did not affect E_{TH} (VERA:-49.72±3 mV; +bithionol:-43.1±6.5 mV; NS). Bithionol effects on V_m and I_{TTX} converge to indicate that, albeit enhanced, I_{KNa} may still depend on I_{NaL} for activation. Put in terms of physiological interaction, these observations suggest that I_{NaL} causes I_{KNa} activation which, in turn, may substantially offset the change in V_m which would result from I_{NaL} alone. By reducing Na^+ driving force, V_m depolarization may actually limit influx through open Na^+ channels; therefore the presence of I_{KNa} is expected to amplify the impact of I_{NaL} on Na^+ influx.

Effect of V_m on I_{NaL}– dependent modulation of intracellular Ca^{2+}

Because cytosolic Na^+ accumulation impairs Ca^{2+} extrusion through the Na/Ca exchanger, I_{KNa} expression might simultaneously blunt the effect of I_{NaL} enhancement on V_m and amplify the one on intracellular Ca^{2+} homeostasis.

To evaluate this hypothesis, the effect of I_{NaL} modulation on intracellular Ca^{2+} was tested while clamping membrane potential to values suitable to simulate the conditions of coupled I_{NaL} - I_{KNa} activation (represented by I_{TTX}) and I_{NaL} activation alone (represented by I_{TTX} + KBK) respectively.

Fluo4-AM (10 μM) loaded INS cells were depolarized for 1 s from a holding potential of -80 mV to potentials respectively negative to I_{TTX} reversal (-10 and 0 mV), and encompassed by I_{TTX} and I_{NaL} reversals (+20 mV) (Fig 5 A). The increments of intracellular Ca^{2+} induced by depolarization were recorded in control and in the

presence of TTX, to block Na^+ influx through I_{Na}. As shown in Fig. 7, TTX reduced the amplitude of Ca^{2+} responses at all the potentials, but its effect was maximal at the intermediate one (Δ%, -10 mV: 9.0±4.1% ; 0 mV: 16.2±1.78 %; 20 mV: 10,1±2.1%). This confirms the expectation that, by preventing V_m to approach I_{NaL} reversal, I_{KNa} may increase I_{NaL} impact on intracellular Ca^{2+} handling.

TTX also accelerated Ca^{2+} decay at -80 mV (τ, Δ%. -10 mV: 20.7±4.5%; 0 mV: 15.6±2.0%; +20 mV: 20.1±2.4%), as expected from an increase in the driving force for the Na/Ca exchanger (NCX). However, in this case, TTX effect did not significantly depend on voltage of the previous step, thus suggesting that voltage-sensitivity of Na/Ca exchange is related to actual Na^+ influx to the sub-sarcolemmal space, rather than to bulk cytosolic Na^+ concentration[26].

I_{NaL} modulation by chronic exposure to high glucose

The above findings indicate that I_{NaL} is normally expressed in β-cells and may thus be involved in their physiology. Nevertheless, as in other tissues, pathophysiological significance of I_{NaL} may require its enhancement under relevant conditions [15;16], which may be represented in this case by chronic exposure to high glucose[27]. Thus, I_{NaL} was evaluated in INS-1E cells incubated for 24h in a medium containing 33 mM glucose (HG)[27]. I_{TTX} was measured under conditions identical to those of non-incubated cells (2.5 mM glucose + 50 μM TOLB), which were used as control (CTRL).

As shown by fig. 8, HG markedly increased I_{TTX} inward amplitude (Mean I_{IN}, CTRL: -3.54±0.48 pA/pF; HG: -8.8±0.92 pA/pF $p<0.05$) and a significant, but small positive shift of E_{REV} (CTRL: 11.2±2.2 mV; HG: 16.12±2.3 mV $p<0.05$). HG tended to shift E_{TH} (CTRL: -

25.9±2.2 mV; HG: -20.8±1.5 mV $p<0.05$) and the voltage at peak I_{TTX} in the positive direction.

Comparison with fig 4 shows remarkable differences between the effects of HG and VERA on I_{TTX}. Whereas the increment of inward component was comparable, HG did not induce the large negative E_{TH} shift caused by VERA, thus indicating that HG may fail to affect the set of low-threshold channels enhanced by VERA. Furthermore, at variance with VERA, HG caused a small positive shift in E_{rev}, thus suggesting comparatively smaller effect on the I_{NaL} /I_{KNa} balance.

Thus, chronic exposure to high glucose markedly enhanced I_{NaL} without disrupting the balance between I_{NaL} and I_{KNa}.

Effect of I_{NaL} modulation on insulin secretion

Glucose-induced insulin secretion was studied in INS1-E preparations (Fig 9)

Under baseline conditions, RAN failed to affect secretion. A trend for a decrease was observed with TTX, but it did not achieve statistical significance. Acute exposure to VERA sharply increased secretion; this effect was completely reversed by concomitant exposure to TTX and significantly blunted by RAN.

Cell incubation for 72 hrs in HG or VERA respectively diminished and abolished the secretory response to high glucose (Fig. 9B). When RAN was added to the HG incubation medium the secretory response was significantly preserved.

Discussion

This study provides information relevant to β-cells physiology: 1) selective I_{NaL} blockade (by RAN) did not prevent TOLB-induced firing and led membrane hyperpolarization only in the presence of I_{NaL} enhancement (by VERA); 2) I_{NaL} was significantly expressed in INS-1E cells under basal conditions and similar to that recorded from human pancreatic islets; 3) I_{NaL} was coupled, through Na^+ influx, to a K^+ conductance (I_{KNa}), putatively mediated by *Slack* channels, whose transcript was highly expressed in INS-1E cells; 4) I_{NaL} affected intracellular Ca^{2+} response to depolarization in a voltage-dependent fashion; 5) I_{NaL} was enhanced by chronic exposure to high glucose, a condition relevant to diabetes.

Effect of I_{NaL} modulation on membrane potential

Action potential firing, induced by tolbutamide, was abolished by TTX, but not by RAN, thus confirming that the latter may selectively block the sustained I_{Na} component , as previously reported in cardiac myocytes and neurons[28;29]. Thus, while inhibiting Na^+ influx through I_{NaL} during sustained depolarization, RAN may not affect Na^+ and Ca^{2+} influx triggered by action potentials.

Further membrane depolarization induced by VERA may result from I_{NaL} enhancement, as indicated by its reversal by TTX and, to a lesser extent, by RAN. Because TTX was applied at a concentration (0.5 μM) blocking "neuronal type" (or TTX-S) Na^+ channels only, the large effect of TTX is consistent with VERA enhancement of I_{NaL} through TTX-S channels isoforms [21]. Nevertheless, the present results suggest that, at variance with RAN-S

ones, RAN-R channels may be weakly coupled to those carrying I_{KNa} (see below) and this may contribute to explain the larger V_m changes associated with their modulation.

Na_V isoforms underlying I_{NaL}

According to RT-PCR measurements, INS-1E cells express transcripts for several TTX-S channels (Nav 1.1 to 1.4, 1.6 and 1.7)[20] and one TTX-R (NaV1.9) isoform. Among TTX-S channels, those known to be sensitive also to RAN (at the concentration used) are Na_V 1.3, 1.4 and 1.7[30-32]. On the other hand, Na_V 1.1 is reportedly resistant to RAN (RAN-R)[33]; however, information concerning the remaining isoforms is missing.

Under basal conditions, I_{TTX} and I_{RAN} differed only in terms of activation threshold (E_{TH}), which was more negative for I_{TTX}. This suggests the presence of a population of low-threshold channels sensitive to TTX, but resistant to RAN.

VERA caused a large negative shift of E_{TH} for I_{TTX} (Fig 4), which may be interpreted either as a gating effect, or as I_{NaL} enhancement through low-threshold TTX-S channels. On the other hand, E_{TH} of I_{RAN} was only slightly hyperpolarized by VERA, thus confirming poor sensitivity to RAN of the subset of TTX-S low-threshold channels. According to the (incomplete) information on TTX vs RAN sensitivity of Na_V isoforms, Na_V 1.1 provides the best fit with the low-threshold, TTX-S and RAN-R pattern. Nevertheless, contribution by Na_V 1.2 and 1.6 cannot be ruled out for lack of information on RAN sensitivity.

Coupling between I_{NaL} and I_{KNa}

Under basal conditions, the reversal potential (E_{rev}) of I_{TTX} and I_{RAN} was largely negative to the value expected for selective Na^+ currents. Non selective blockade of K^+ channels (KBK solution) strongly shifted E_{rev}, to approach the expected Na^+ equilibrium potential (Fig 5). Altogether these findings indicate that I_{TTX} and I_{RAN} included a component carried by a K^+ channel; *i.e.* they were composite I_{NaL} + I_{KNa} currents. Because TTX does not directly block K^+ channels, this component must reflect a Na^+-activated K^+ conductance (I_{KNa}). This argument might not hold for RAN, which directly blocks ERG-type K^+ current (I_{ERG}) at the concentration used [22]; however, selective I_{ERG} blockade (by E-4031) had negligible effect on membrane current recorded during the ramp protocol (Supplement Fig 3), possibly because of extensive I_{ERG} inactivation during slow depolarizations. Thus, also in the case of I_{RAN}, the steady-state outward component may largely reflect I_{KNa}.

Unfortunately, the KBK solution also reduced I_{TTX} and I_{RAN} inward amplitudes, thus implying ancillary I_{Na} blockade, a reported effect of 4-AP[34;35]. While this ancillary effect cannot account for the observed E_{rev} changes, it prevents interpretation of E_{TH} changes in terms of K^+ channel blockade. More solid information on the correspondence of I_{KNa} activation with Na^+ influx can be provided by the effect of the selective I_{KNa} activator bithionol. As shown in fig 6B, albeit strongly shifting the E_{rev} of I_{TTX} , bithionol failed to change its E_{TH}. This implies that I_{KNa} activation was closely coupled to that of I_{NaL}, *i.e.* to Na^+ influx.

I_{NaL} enhancement by VERA (fig 4) and chronic exposure to high glucose (HG, Fig 8) significantly shifted the voltages at I_{TTX} peak and reversal, but failed to modify the same parameters in the case of I_{RAN}. Absence of changes in the voltage dependency of the composite I_{NaL}+I_{KNa} current upon I_{NaL} enhancement suggests strong coupling between the Na^+ and K^+ components. Thus, the Na^+ channel isoforms blocked by RAN may be more closely coupled to I_{KNa} channels than RAN-R ones. Comparison of available data on drug sensitivity and activation threshold [20] suggests that, among the Na_V isoforms detected by rt-PCR, the best candidate for coupling with I_{KNa} channels was Na_V 1.3 (highly expressed, RAN-S and higher threshold).

Coupling to I_{KNa} conceivably limits the impact of I_{NaL} on V_m, and this may explain why, in spite of clearly detectable I_{NaL} under basal conditions, V_m was not hyperpolarized by its selective blockade (Fig 1). Ancillary I_{ERG} blockade by RAN [22] might theoretically contribute to limit its impact on V_m; however, the negligible effect of E-4031 on ramp current (suppl Fig 3) suggests that I_{ERG} may be almost completely inactivated during sustained depolarization. On the other hand, failure of V_m to depolarize in response to Na^+ channels opening may actually enhance the driving force for Na^+ influx, thus increasing the impact of I_{NaL} enhancement on intracellular ionic homeostasis. This view is supported by the observation that the effect of I_{NaL} blockade on intracellular Ca^{2+} was maximal at intermediate potentials. Nevertheless, V_m restrain by I_{KNa} might also blunt auto-regenerative I_{Na} activation; thus, its net effect on Na^+ influx may ultimately depend on the position of V_m relative to I_{Na} activation

curve (enhancement prevailing at more positive V_m , where Na^+ driving force becomes the limiting factor).

The expression of channels potentially accounting for I_{KNa} was investigated by rt-PCR and transcripts for both *Slick* and *Slack* proteins were identified. These, channels, originally described in dorsal root ganglia[36], are expressed throughout the nervous system [37;38]. Tight functional coupling between I_{NaL} and I_{KNa} has been previously described in central neurons [39] and recently confirmed by excised-patch recordings in olfactory neurons [40]. These findings converge to suggest that channel co-localization may underlie the crosstalk between channels. Although the present data do not include evidence of channel co-localization, strict coupling is indicated by the close match between I_{NaL} and I_{KNa} in terms of voltage-dependency and sensitivity to blockade.

Similar levels of *Slack* and *Slick* transcripts were detected by RT-PCR.; thus, both isoforms might contribute to I_{KNa} . However, whereas *Slick* channel activation requires high intracellular Cl^- and is inhibited by ATP[41], a low Cl^- - high ATP pipette solution was used; moreover, only the *Slack* isoform is sensitive to bithionol. Therefore, *Slack* is a better candidate for supporting I_{KNa} in INS-1E cells. Albeit clearly detectable, transcript levels of each isoform were in the intermediate-low range if compared with K_{IR} 6.2, which can be viewed as positive reference. Nevertheless, it should be considered that the encoded channels have a large unitary conductance[23]; thus, they may support a functionally significant current even at low expression levels.

Na^+ -activated K^+ channels bear a functional analogy with Ca^{2+}-activated ones [37;42], which are involved in generating periodical burst activity in neurons[36;41]. Thus, it can be hypothesized that I_{KNa} may also contribute to the oscillatory response of V_m to glucose challenge in pancreatic β-cells.

I_{NaL} is enhanced by long-term exposure to high glucose

A novel finding of this work is the enhancement of I_{TTX} and I_{RAN} after chronic exposure to high glucose levels (HG, 33 mM, Fig. 8). Both the inward and the outward component of these currents were enhanced by HG, thus preserving the I_{NaL} /I_{KNa} balance. I_{NaL} is linked to Ca^{2+} homeostasis, which may thus be chronically perturbed by HG-induced I_{NaL} enhancement. In cardiac myocytes, I_{NaL} enhancement boosts function (force development) acutely but, on the long run, it strongly contributes to failure[43]; the same paradigm might apply to β-cells. Indeed, long term Ca^{2+} overload might impair glucose-induced insulin secretion functionally (*e.g.* by causing fasting insulin leak) and affect β-cell survival by facilitating apoptosis. The observation that RAN prevented β-cell loss in mice with streptozotocin-induced diabetes[6] is in line with this view.

The evidence collected thus far in different tissues suggests that I_{NaL} enhancement may represent a widespread response to stress[43;44], ultimately operated by CaMKII-dependent channel phosphorylation, but initiated by a variety of stimuli, including redox imbalance[7;45]. Accumulation of reactive oxygen species (ROS) is an important mechanism in streptozotocin-induced damage[46] and is also among the consequences of chronic exposure to high glucose[47]. Thus,

we speculate that ROS accumulation might be involved in HG-induced I_{NaL} enhancement.

Modulation of insulin secretion

Na^+ channels were first described in pancreatic β-cells in 1977 [48]; nevertheless, their functional impact on glucose stimulated insulin secretion (GSIS) is still debated.

Theoretically, I_{Na} might contribute to the voltage-triggered component of insulin secretion in two ways: 1) its transient component (I_{NaT}) may support action potential firing, required for Ca^{2+} influx through high threshold Ca^{2+} channels; 2) Na^+ influx, also supported by non-inactivating components (I_{NaL}) potentially unrelated to action potential firing, may contribute to Ca^{2+} loading through the Na^+/Ca^{2+} exchanger (NCX). In murine β-cells up to 90% of Na^+ channels are inactivated even at membrane potentials occurring in low glucose (about -70 mV)[49]. On the other hand, recent studies in mice β cells demonstrated that I_{Na} inactivation curve is positively shifted by intracellular ATP[50]; thus, high glucose might partially recover Na^+ channel availability. Moreover, Braun et al.[3] recorded sizable I_{NaT} at a holding potential of -70 mV in human β-cells. Overall, action potential firing may not be essential for V-triggered insulin secretion[51], its quantitative contribution is debated and possibly species-dependent. Indeed, TTX (at concentrations blocking TTX-S channels only) had negligible effects on GSIS from mice pancreatic islets[52], but inhibited GSIS from canine and human islets [13].

Insulin secretion was found to be positively correlated with intracellular Na^+ levels during acute exposure to a range of

experimental conditions (I_{Na} blockade, low Na^+ or Na^+/K^+ pump blockade)[3;13;48]. This is expected from the link between cellular Na^+ and Ca^{2+} regulation, the role of Ca^{2+} in modulating secretion and is apparently opposite to what needed to explain the improvement of glycaemic control in RAN-treated diabetic patients[5].

In the present experiments under baseline conditions, RAN did not affect glucose-induced secretion and, although a trend was present, TTX effect did not achieve significance (Fig. 9). While the method and sample size used may be inadequate to detect small secretion changes, RAN ineffectiveness is consistent with its failure to affect glycaemia in normal subjects [5],probably related to "normal" I_{NaL} magnitude and lack of effect on action potential firing.

Secretion enhancement by acute exposure to VERA is again consistent with previous knowledge and its reversal by TTX and RAN provides further proof that I_{NaL} enhancement is involved. VERA modulation of TTX-S channels and the observation that these may be partly insensitive to RAN may explain why TTX was more effective in this action.

Notably, after 72 hrs of exposure to either VERA or HG, glucose-induced secretion was strongly blunted, an effect opposed by adding RAN to the incubation medium. Thus the effects of acute and chronic I_{NaL} modulation on secretion were opposite. This indicates that long-term I_{NaL} enhancement may impair β-cell function/survival, a finding reminiscent of the "remodelling" role of I_{NaL} described in cardiac muscle[43] and potentially suitable to explain the beneficial effects of RAN on glycaemic control of diabetic patients. Of course, this does not rule out the possibility that RAN may also modulate the

function of glucagon-secreting cells in a direction contributing to restore balance under conditions of insulin deficiency.

Limitations

The majority of experiments in this study were performed on rat INS-1E cells and extrapolation to native β-cells may require caution. Nevertheless, we compared I_{NaL} recordings between INS-1E cells and cells acutely dissociated from normal human islets (most likely to represent β-cells) and found them superimposable (Supplemental data). Furthermore, the pattern of V_m response to glucose challenge of INS-1E cells (Supplemental data) was similar to that classically described for islet β-cells [53]. The choice to use a pure β-cell preparation (as INS-1E) was motivated by the difficulty in discriminating cell types in islet preparations and to rule out paracrine crosstalk between cell types in secretion studies.

I_{KATP} blockade (by tolbutamide), rather than glucose, was used as the inducing stimulus in the majority of experiments (except for secretion studies). It is fair to stress that the two stimuli may differ because, whereas the latter may involve metabolic mechanisms, the former acts downstream and is purely electrophysiological. At the same time, the study focused on an electrophysiological mechanism (a transmembrane current); thus, the use of tolbutamide is justified by the need to facilitate interpretation of findings. In V-clamp experiments I_{KATP} blockade was further motivated by the need to remove even small fluctuations in background current, potentially contaminating measurement of I_{NaL} by subtraction (as in I_{TTX} or I_{RAN}).

Conclusions and translational relevance

The present findings demonstrate the presence of I_{NaL} in insulin-secreting cells, and its functional coupling with I_{KNa}, with consequences relevant to the electrophysiological component (*i.e.* the "early phase") of secretion control. I_{NaL}-I_{KNa} coupling might exist in other cell types, including glucagon-secreting ones, thus opening the possibility that it may participate in glycaemic control by additional mechanisms. Unveiling the impact of the I_{NaL}/I_{KNa} balance on the physiology of intact islets might disclose new therapeutic approaches to secretion deficiency. Moreover, the present findings show that I_{NaL} enhancement may result from long term exposure to high glucose and adversely affects insulin secretion. This provides at least one mechanistic interpretation of the beneficial effects of I_{NaL} blockade in patients with type 2 diabetes.

Acknowledgements

We thank dr. Claes Wollheim and collaborators for the kind gift of INS-1E cell line. This work was funded by Gilead, Inc (CA) and the Network Enabled Drug Design (NEDD).

Figures

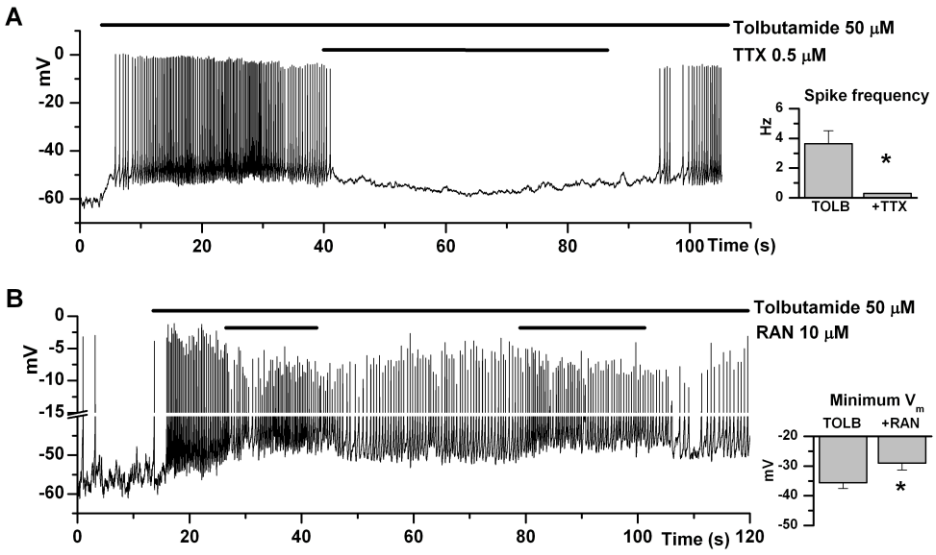

Fig. 1 Effect of I_{NaL} blockers on V_m. Representative gap-free V_m recordings. Test substances applied as indicated by bars. Similar results were obtained for 6 cells (TTX, panel **A**) and 7 cells (RAN, panel **B**).

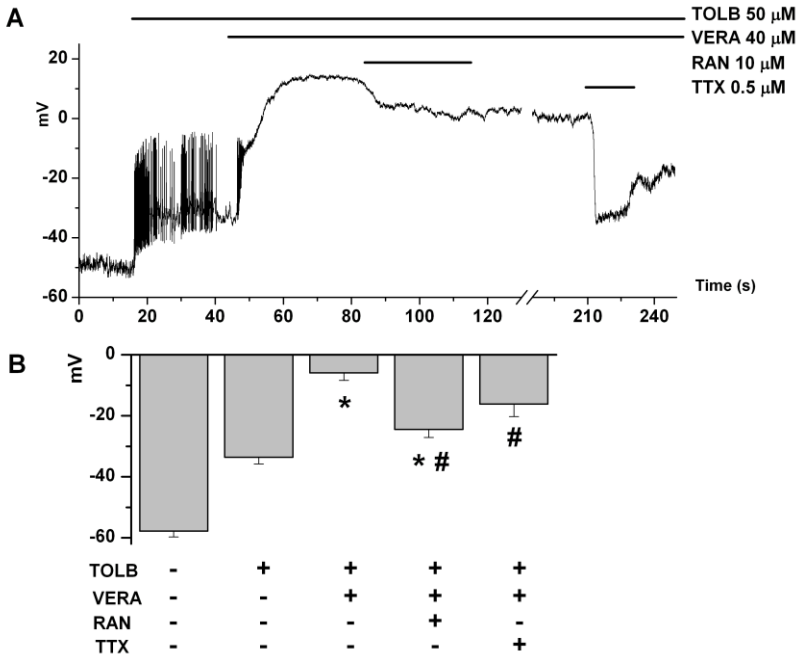

Fig. 2 Effect of I_{NaL} enhancement and blockade on V_m. A Representative gap-free V_m recordings during exposure to interventions, as indicated by bars. Similar traces were obtained for 7 cells (VERA+TTX) and 11 cells (VERA+RAN). **B** Statistics of V_m. TOLB values refer to the mean V_m in the absence of firing *= $p<0.05$ vs TOLB, # =$p<0.05$ vs VERA

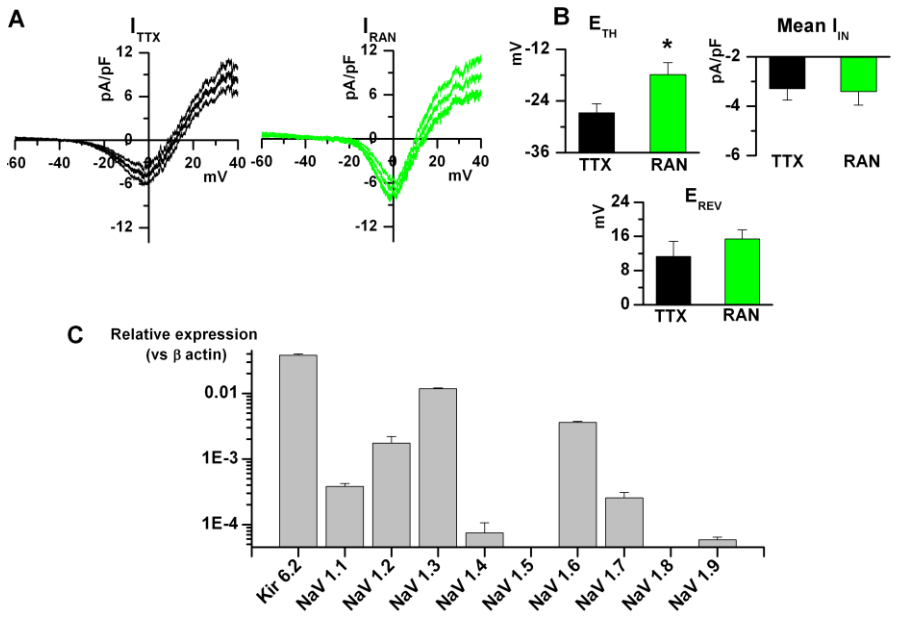

Fig. 3 I_{TTX} and I_{RAN} under baseline conditions A Mean steady-state I/V relationship (± confidence intervals) of I_{TTX} and I_{RAN} (N I_{TTX}: 16; I_{RAN}: 11) **B** Statistics for key parameters of steady-state I/V relationships. E_{TH}: threshold potential; Mean I_{IN}: mean inward current; E_{REV}: reversal potential. * = $p<0.05$ vs TTX **C** Relative mRNA level expression (vs β actin) of NaV channel isoforms. The K_{ATP} channel α subunit K_{IR} 6.2 was used as positive control. Experiments were run in triplicates.

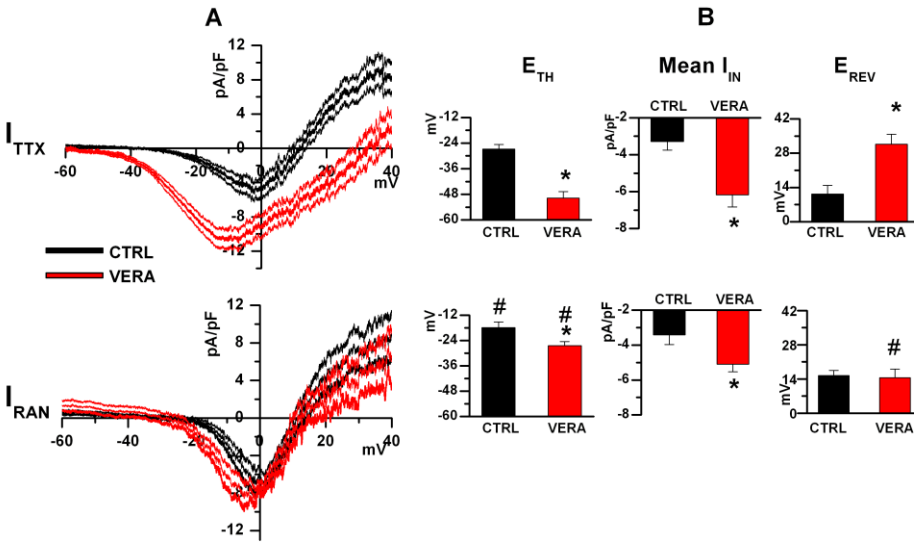

Fig. 4 Effect of I_{NaL} enhancement by VERA on I_{TTX} and I_{RAN}.

A Mean steady-state I/V relationships (± confidence intervals) of I_{TTX} and I_{RAN} in control and after exposure to 40 μM veratridine (VERA) (N I_{TTX}: CTRL:16, VERA: 11; I_{RAN} CTRL:11, VERA: 7) **B** Statistics for key parameters of steady-state I/V relationships, abbreviations as in Fig 1. * = $p<0.05$ vs CTRL. # = $p<0.05$ vs TTX

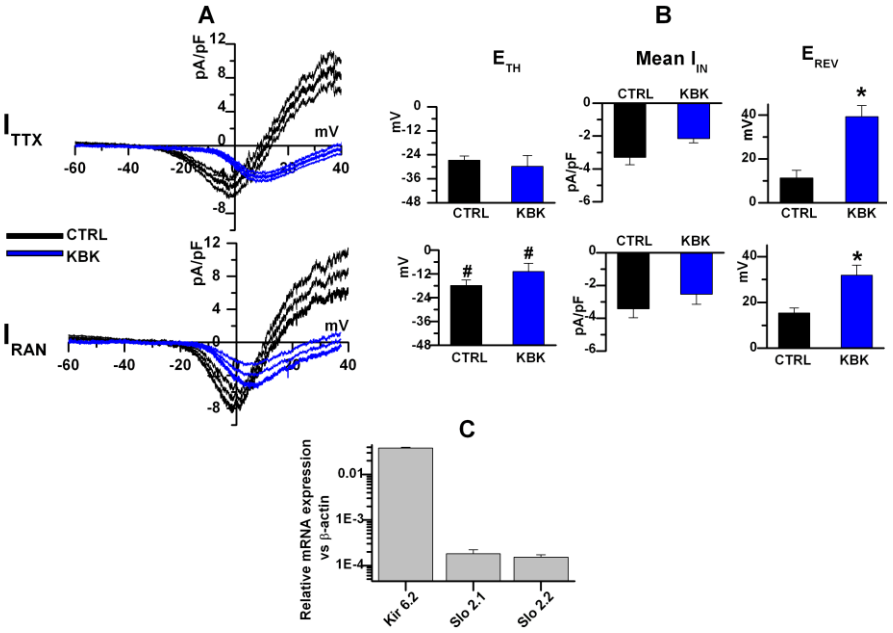

Fig. 5 Effect of K^+ channel blockade (KBK) on I_{TTX} and I_{RAN}.

A Mean steady-state I/V relationship (± confidence intervals) of I_{TTX} and I_{RAN} in control and in presence of 10 mM TEA-chloride and 0.5 μM 4-aminopyridine (KBK) (N I_{TTX}: CTRL:16, KBK: 9; I_{RAN} CTRL:11, KBK: 7). **B** Statistics for key parameters of steady-state I/V relationships, abbreviations as in Fig 1. * = $p<0.05$ vs CTRL. # = $p<0.05$ vs TTX **C** Relative mRNA level expression (vs β actin) of *SLICK* (Slo2.1) and *SLACK* (Slo2.2) The K_{ATP} channel α subunit K_{IR} 6.2 was used as positive control. Experiments were run in triplicates.

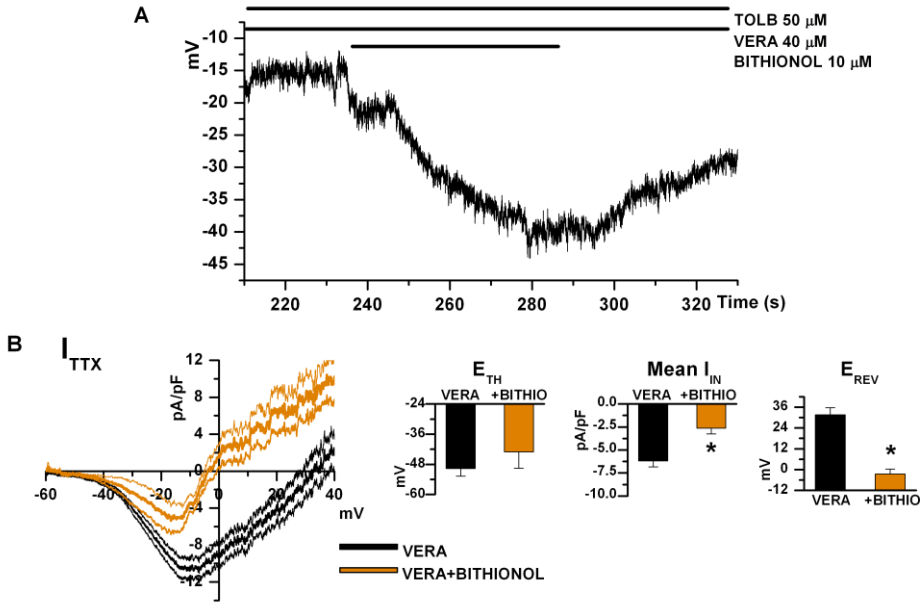

Fig. 6 Effect of I_{KNa} activation on V_m and I_{TTX}.

A Representative trace of gap free recordings of V_m. 10 µM bithionol was superimposed on TOLB and VERA at the time indicated. Similar traces were recorded in 7 cells.

B Up, mean I/V relationship (± confidence intervals) of I_{TTX} in VERA and after addition of 10 µM bithionol. Bottom, quantitative analysis. E_{TH}: threshold potential; Mean I_{IN}: Mean inward current; E_{REV}: reversal potential. (N VERA:16, +BITHIO: 9)

* = $p<0.05$ vs CTRL.

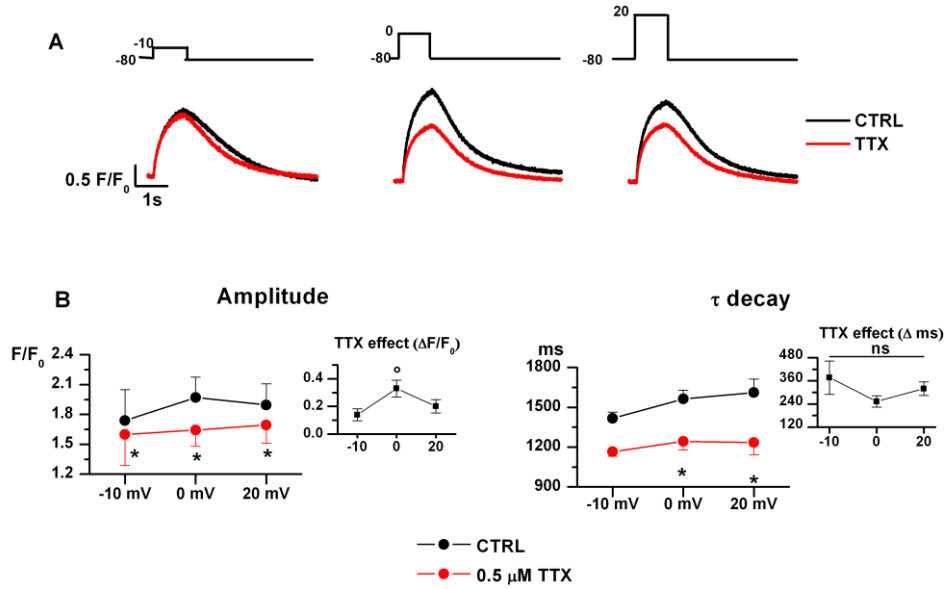

Fig. 7 TTX effect on V-evoked Ca^{2+} increments.

A Representative traces of V-evoked Ca^{2+} responses at three different test potentials, as shown in the V-clamp protocols above (time-aligned).

B Statistics for TTX effect on V-induced Ca^{2+} responses; TTX-induced changes are shown in the insets. Left: amplitude; Right: decay time constants (τ). (N=7 for each potential). * = $p<0.05$ vs CTRL

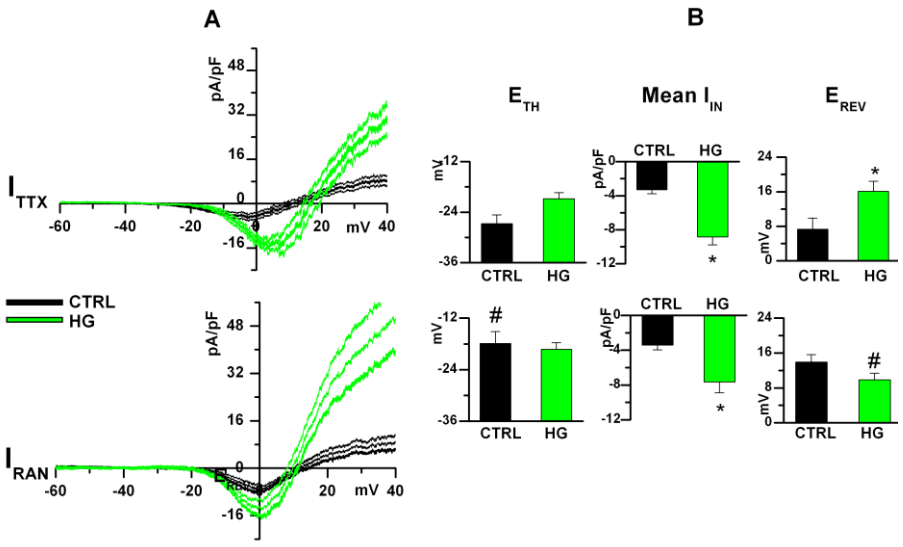

Fig. 8 I_{TTX} and I_{RAN} after chronic exposure to 33 mM glucose (HG).

A Mean steady-state I/V relationships (± confidence intervals) of I_{TTX} and I_{RAN} in control and after 24 h exposure to 33 mM glucose (HG) (N, TTX CTRL: 16; HG: 9 ; RAN CTRL: 11; HG:11)

B Statistics for key parameters of steady-state I/V relationships, abbreviations as in Fig 1. * = $p<0.05$ vs CTRL. #=$p<0.05$ vs TTX

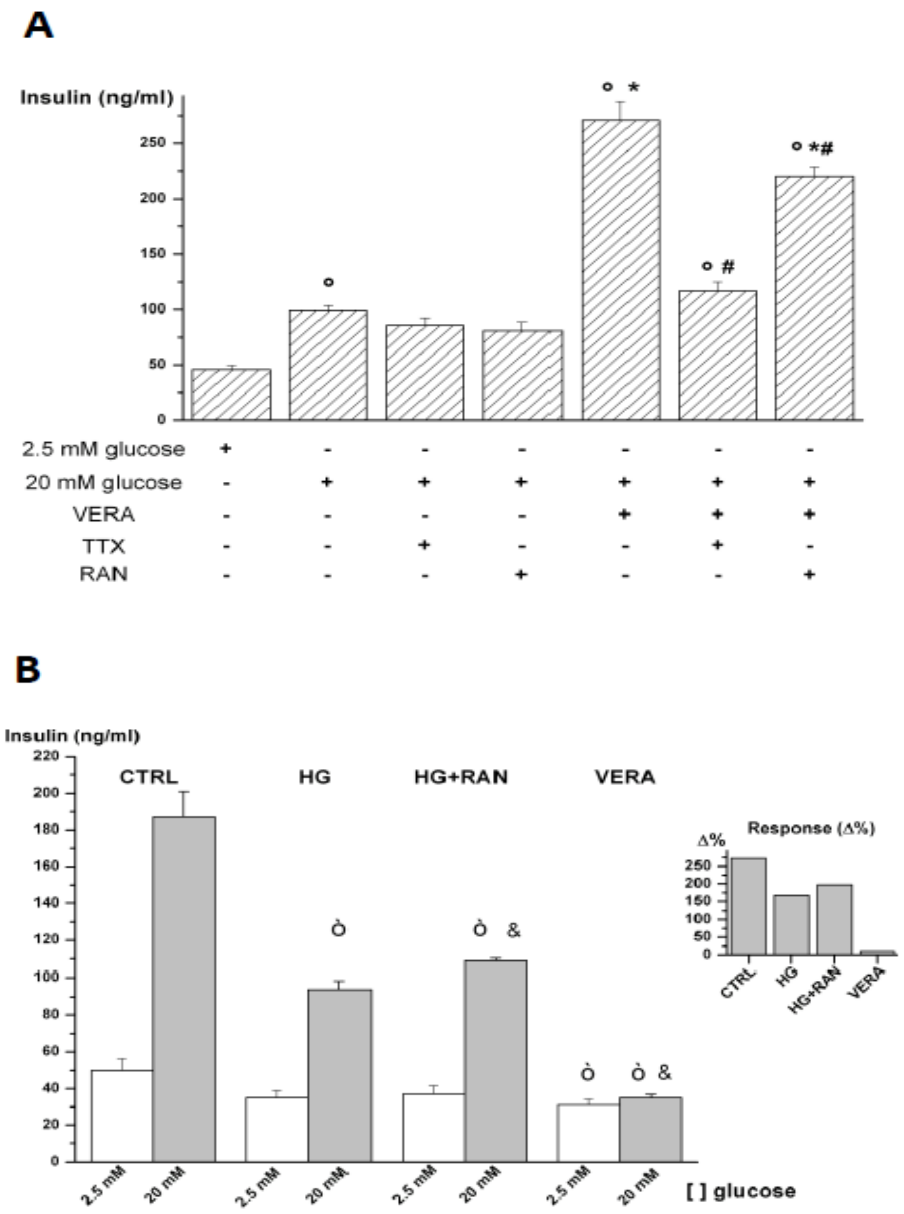

Fig. 9 Effect of I_{NaL} modulators on GSIS A Insulin secretion after acute exposure (1h) to the test substances (N=9) ° = p<0.05 vs 2.5 mM glucose; *= p<0.05 vs 20 mM glucose; #=p<0.05 vs vera

B Response to glucose challenge after chronic (72 hrs) exposure to the conditions indicated (CTRL: normal glucose; HG: 33 mM glucose; HG + RAN: 33 μM glucose + 10 mM RAN; VERA: 40 μM veratridine). For each intervention secretions in 2.5 and 20 mM glucose are compared.. The inset shows the % effect of glucose challenge. N= 9 for each group; ò=p<0.05 vs CTRL; &=p<0.05 vs HG.

Supplementary material

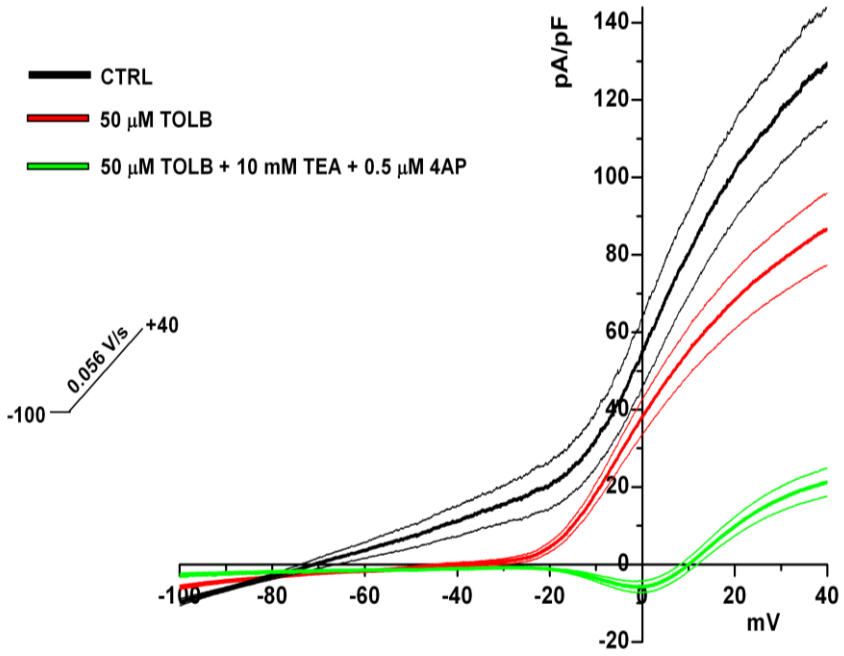

Fig. S1 Total steady-state I/V relationship of INS-1E cells. Mean steady-state I/V relationship of total membrane current (± confidence intervals) in INS-1E cells. Measurements were made in perforated patch to avoid disturbances in intracellular environment. (N, CTRL: 12, TOLB: 11, TOLB+TEA+4AP: 12)

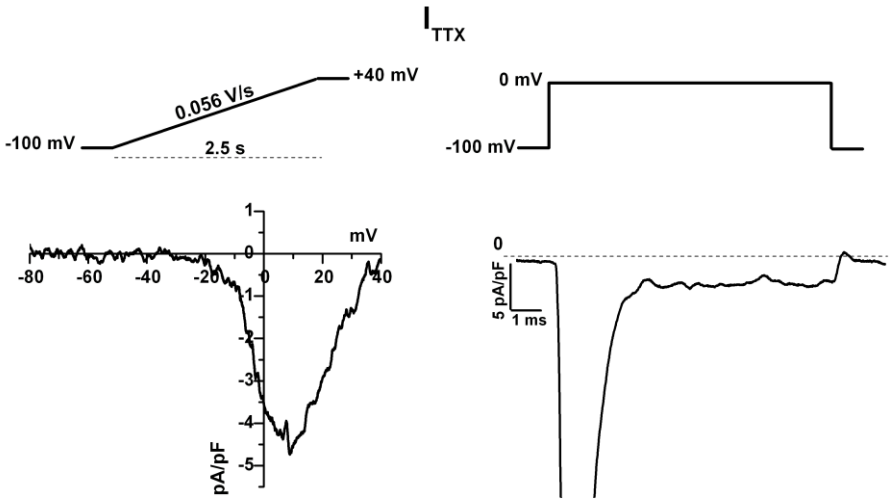

Fig. S2 Equivalence between I_{NaL} measurement by ramp and step protocols. Example of I_{TTX} recorded from the same cell during whole-cell conditions. Recordings performed in the presence of 50 μM TOLB, 10 mM TEA and 0.5 μM 4AP (KBK solution).

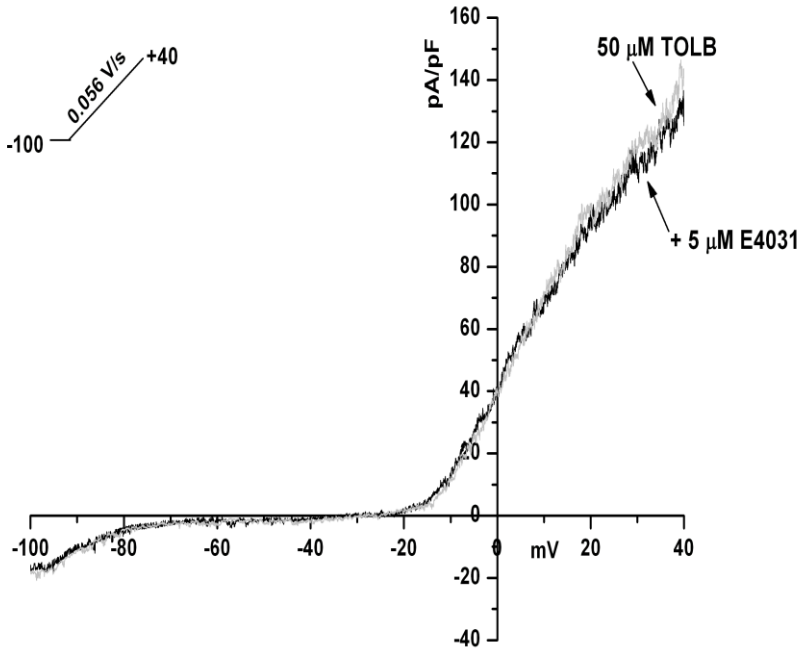

Fig. S3 E4031 effect on ramp currents. Representative recording; similar results in 5 cells.

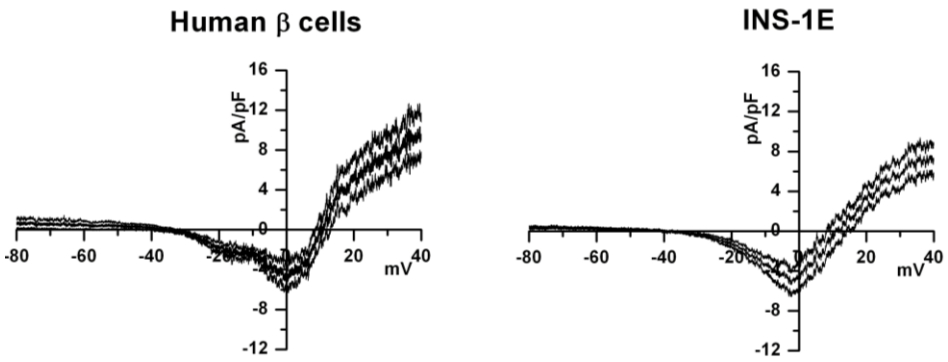

Fig. S4 Comparison between I_{TTX} in INS-1E cells and human pancreatic β-cells (freshly isolated from islets). Average traces ± SE (N = 7 for human and 16 for INS-1E)

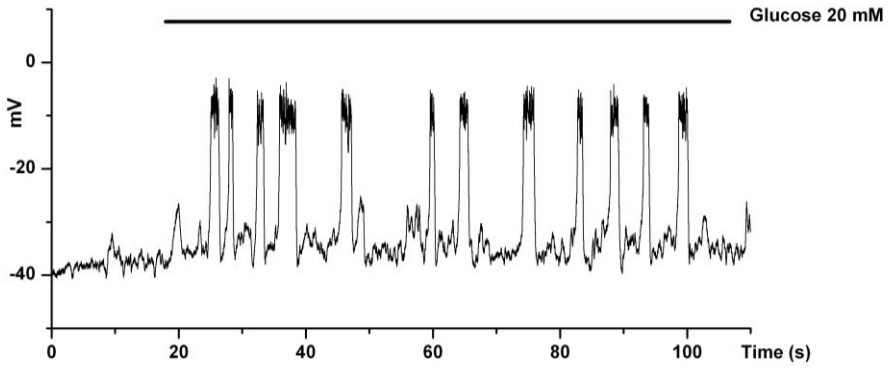

Fig. S5 Glucose effect on V_m in INS-1E cells. Representative gap free recording of electrical activity elicited by 20 mM glucose in INS-1E cells. Similar traces were obtained in 8 cells.

Reference List of Chapter 2

1. Nesher R, Anteby E, Yedovizky M, Warwar N, Kaiser N, Cerasi E. Beta-cell protein kinases and the dynamics of the insulin response to glucose. *Diabetes*. 2002;51 Suppl 1:S68-S73.

2. Wang Z, Thurmond DC. Mechanisms of biphasic insulin-granule exocytosis - roles of the cytoskeleton, small GTPases and SNARE proteins. *J Cell Sci*. 2009;122:893-903.

3. Braun M, Ramracheya R, Bengtsson M, Zhang Q, Karanauskaite J, Partridge C, Johnson PR, Rorsman P. Voltage-gated ion channels in human pancreatic beta-cells: electrophysiological characterization and role in insulin secretion. *Diabetes*. 2008;57:1618-1628.

4. Eberhardson M, Grapengiesser E. Role of voltage-dependent Na+ channels for rhythmic Ca2+ signalling in glucose-stimulated mouse pancreatic beta-cells. *Cell Signal*. 1999;11:343-348.

5. Chisholm JW, Goldfine AB, Dhalla AK, Braunwald E, Morrow DA, Karwatowska-Prokopczuk E, Belardinelli L. Effect of ranolazine on A1C and glucose levels in hyperglycemic patients with non-ST elevation acute coronary syndrome. *Diabetes Care*. 2010;33:1163-1168.

6. Ning Y, Zhen W, Fu Z, Jiang J, Liu D, Belardinelli L, Dhalla AK. Ranolazine increases beta-cell survival and improves glucose homeostasis in low-dose streptozotocin-induced diabetes in mice. *J Pharmacol Exp Ther*. 2011;337:50-58.

7. Song Y, Shryock JC, Wagner S, Maier LS, Belardinelli L. Blocking late sodium current reduces hydrogen peroxide-induced arrhythmogenic activity and contractile dysfunction. *J Pharmacol Exp Ther*. 2006;318:214-222.

8. Saint DA. The role of the persistent Na(+) current during cardiac ischemia and hypoxia. *J Cardiovasc Electrophysiol*. 2006;17 Suppl 1:S96-S103.

9. Tang Q, Ma J, Zhang P, Wan W, Kong L, Wu L. Persistent sodium current and Na+/H+ exchange contributes to the augmentation of the reverse Na+/Ca2+ exchange during hypoxia or acute ischemia in ventricular myocytes. *Pflugers Arch*. 2012;463:513-522.

10. Dionne KE, Colton CK, Yarmush ML. Effect of hypoxia on insulin secretion by isolated rat and canine islets of Langerhans. *Diabetes*. 1993;42:12-21.

11. Chen WJ, Liu XY, Wang LX, Wang YP, Liu XH, Liu LB. [Oxidative damage to the endoplasmic reticulum stress pathway of apoptosis-related molecules expression in MIN6 cell]. *Xi Bao Yu Fen Zi Mian Yi Xue Za Zhi*. 2011;27:249-52, 256.

12. Wang M, Crager M, Pugazhenthi S. Modulation of apoptosis pathways by oxidative stress and autophagy in beta cells. *Exp Diabetes Res*. 2012;2012:647914.

13. Barnett DW, Pressel DM, Misler S. Voltage-dependent Na+ and Ca2+ currents in human pancreatic islet beta-cells: evidence for

roles in the generation of action potentials and insulin secretion. *Pflugers Arch*. 1995;431:272-282.

14. Pressel DM, Misler S. Sodium channels contribute to action potential generation in canine and human pancreatic islet B cells. *J Membr Biol*. 1990;116:273-280.

15. Belardinelli L, Shryock JC, Fraser H. Inhibition of the late sodium current as a potential cardioprotective principle: effects of the late sodium current inhibitor ranolazine. *Heart*. 2006;92 Suppl 4:iv6-iv14.

16. Undrovinas A, Maltsev VA. Late sodium current is a new therapeutic target to improve contractility and rhythm in failing heart. *Cardiovasc Hematol Agents Med Chem*. 2008;6:348-359.

17. Undrovinas NA, Maltsev VA, Belardinelli L, Sabbah HN, Undrovinas A. Late sodium current contributes to diastolic cell Ca2+ accumulation in chronic heart failure. *J Physiol Sci*. 2010;60:245-257.

18. Ye J, Coulouris G, Zaretskaya I, Cutcutache I, Rozen S, Madden TL. Primer-BLAST: a tool to design target-specific primers for polymerase chain reaction. *BMC Bioinformatics*. 2012;13:134.

19. Livak KJ, Schmittgen TD. Analysis of relative gene expression data using real-time quantitative PCR and the 2(-Delta Delta C(T)) Method. *Methods*. 2001;25:402-408.

20. Catterall WA, Goldin AL, Waxman SG. International Union of Pharmacology. XXXIX. Compendium of voltage-gated ion channels: sodium channels. *Pharmacol Rev*. 2003;55:575-578.

21. Farrag KJ, Bhattacharjee A, Docherty RJ. A comparison of the effects of veratridine on tetrodotoxin-sensitive and tetrodotoxin-resistant sodium channels in isolated rat dorsal root ganglion neurons. *Pflugers Arch*. 2008;455:929-938.

22. Rajamani S, Shryock JC, Belardinelli L. Rapid kinetic interactions of ranolazine with HERG K+ current. *J Cardiovasc Pharmacol*. 2008;51:581-589.

23. Aoki K, Kosakai K, Yoshino M. Monoaminergic modulation of the Na+-activated K+ channel in Kenyon cells isolated from the mushroom body of the cricket (Gryllus bimaculatus) brain. *J Neurophysiol*. 2008;100:1211-1222.

24. Kim YC, Sim JH, Kang TM, Suzuki H, Kim SR, Kwon SC, Xu WX, Lee SJ, Kim KW. Sodium-activated potassium current in guinea pig gastric myocytes. *J Korean Med Sci*. 2007;22:57-62.

25. Yang B, Gribkoff VK, Pan J, Damagnez V, Dworetzky SI, Boissard CG, Bhattacharjee A, Yan Y, Sigworth FJ, Kaczmarek LK. Pharmacological activation and inhibition of Slack (Slo2.2) channels. *Neuropharmacology*. 2006;51:896-906.

26. Weber CR, Ginsburg KS, Bers DM. Cardiac submembrane [Na+] transients sensed by Na+-Ca2+ exchange current. *Circ Res*. 2003;92:950-952.

27. Wang Y, Gao L, Li Y, Chen H, Sun Z. Nifedipine Protects INS-1 beta-Cell from High Glucose-Induced ER Stress and Apoptosis. *Int J Mol Sci*. 2011;12:7569-7580.

28. Hasenfuss G, Maier LS. Mechanism of action of the new anti-ischemia drug ranolazine. *Clin Res Cardiol*. 2008;97:222-226.

29. Nodera H, Rutkove SB. Long-term nerve excitability changes by persistent Na+ current blocker ranolazine. *Neurosci Lett*. 2012;524:101-106.

30. Hirakawa R, El Bizri N, Shryock JC, Belardinelli L, Rajamani S. Block of Na+ currents and suppression of action potentials in embryonic rat dorsal root ganglion neurons by ranolazine. *Neuropharmacology*. 2012;62:2251-2260.

31. Rajamani S, Shryock JC, Belardinelli L. Block of tetrodotoxin-sensitive, Na(V)1.7 and tetrodotoxin-resistant, Na(V)1.8, Na+ channels by ranolazine. *Channels (Austin)*. 2008;2:449-460.

32. Wang GK, Calderon J, Wang SY. State- and use-dependent block of muscle Nav1.4 and neuronal Nav1.7 voltage-gated Na+ channel isoforms by ranolazine. *Mol Pharmacol*. 2008;73:940-948.

33. Kahlig KM, Lepist I, Leung K, Rajamani S, George AL. Ranolazine selectively blocks persistent current evoked by epilepsy-associated Nanu1.1 mutations. *Br J Pharmacol*. 2010;161:1414-1426.

34. Lu BX, Liu LY, Liao L, Zhang ZH, Mei YA. Inhibition of Na+ channel currents in rat myoblasts by 4-aminopyridine. *Toxicol Appl Pharmacol*. 2005;207:275-282.

35. Mei YA, Wu MM, Huan CL, Sun JT, Zhou HQ, Zhang ZH. 4-aminopyridine, a specific blocker of K(+) channels, inhibited inward Na(+) current in rat cerebellar granule cells. *Brain Res*. 2000;873:46-53.

36. Gao SB, Wu Y, Lu CX, Guo ZH, Li CH, Ding JP. Slack and Slick KNa channels are required for the depolarizing afterpotential of acutely isolated, medium diameter rat dorsal root ganglion neurons. *Acta Pharmacol Sin*. 2008;29:899-905.

37. Bhattacharjee A, Gan L, Kaczmarek LK. Localization of the Slack potassium channel in the rat central nervous system. *J Comp Neurol*. 2002;454:241-254.

38. Bhattacharjee A, von Hehn CA, Mei X, Kaczmarek LK. Localization of the Na+-activated K+ channel Slick in the rat central nervous system. *J Comp Neurol*. 2005;484:80-92.

39. Budelli G, Hage TA, Wei A, Rojas P, Jong YJ, O'Malley K, Salkoff L. Na+-activated K+ channels express a large delayed outward current in neurons during normal physiology. *Nat Neurosci*. 2009;12:745-750.

40. Hage TA, Salkoff L. Sodium-activated potassium channels are functionally coupled to persistent sodium currents. *J Neurosci*. 2012;32:2714-2721.

41. Bhattacharjee A, Joiner WJ, Wu M, Yang Y, Sigworth FJ, Kaczmarek LK. Slick (Slo2.1), a rapidly-gating sodium-activated potassium channel inhibited by ATP. *J Neurosci*. 2003;23:11681-11691.

42. Nuwer MO, Picchione KE, Bhattacharjee A. cAMP-dependent kinase does not modulate the Slack sodium-activated potassium channel. *Neuropharmacology*. 2009;57:219-226.

43. Zaza A, Belardinelli L, Shryock JC. Pathophysiology and pharmacology of the cardiac "late sodium current.". *Pharmacol Ther*. 2008;119:326-339.

44. Ma J, Luo A, Wu L, Wan W, Zhang P, Ren Z, Zhang S, Qian C, Shryock JC, Belardinelli L. Calmodulin kinase II and protein kinase C mediate the effect of increased intracellular calcium to augment late sodium current in rabbit ventricular myocytes. *Am J Physiol Cell Physiol*. 2012;302:C1141-C1151.

45. Qian C, Ma J, Zhang P, Luo A, Wang C, Ren Z, Kong L, Zhang S, Wang X, Wu Y. Resveratrol attenuates the Na(+)-dependent intracellular Ca(2+) overload by inhibiting H(2)O(2)-induced increase in late sodium current in ventricular myocytes. *PLoS One*. 2012;7:e51358.

46. Szkudelski T. The mechanism of alloxan and streptozotocin action in B cells of the rat pancreas. *Physiol Res*. 2001;50:537-546.

47. Kaneto H, Katakami N, Matsuhisa M, Matsuoka TA. Role of reactive oxygen species in the progression of type 2 diabetes and atherosclerosis. *Mediators Inflamm*. 2010;2010:453892.

48. Donatsch P, Lowe DA, Richardson BP, Taylor P. The functional significance of sodium channels in pancreatic beta-cell membranes. *J Physiol*. 1977;267:357-376.

49. Lou XL, Yu X, Chen XK, Duan KL, He LM, Qu AL, Xu T, Zhou Z. Na+ channel inactivation: a comparative study between pancreatic islet beta-cells and adrenal chromaffin cells in rat. *J Physiol*. 2003;548:191-202.

50. Zou N, Wu X, Jin YY, He MZ, Wang XX, Su LD, Rupnik M, Wu ZY, Liang L, Shen Y. ATP regulates sodium channel kinetics in pancreatic islet Beta cells. *J Membr Biol*. 2013;246:101-107.

51. Hatlapatka K, Willenborg M, Rustenbeck I. Plasma membrane depolarization as a determinant of the first phase of insulin secretion. *Am J Physiol Endocrinol Metab*. 2009;297:E315-E322.

52. Meissner HP, Schmelz H. Membrane potential of beta-cells in pancreatic islets. *Pflugers Arch*. 1974;351:195-206.

53. Merglen A, Theander S, Rubi B, Chaffard G, Wollheim CB, Maechler P. Glucose sensitivity and metabolism-secretion coupling studied during two-year continuous culture in INS-1E insulinoma cells. *Endocrinology*. 2004;145:667-678.

CHAPTER 3 – CONCLUSIONS

The findings reported in Chapter 2 can be summarized as follows:

1) Pancreatic β cells express a sizable I_{NaL}, which is sensitive to both TTX and RAN blockade.
2) The impact of I_{NaL} on V_m is negligible in normal conditions, but become more relevant when the current is pharmacologically enhanced (by VERA).
3) The effects of TTX and RAN on V_m were compatible with the I/V relationships of I_{TTX} and I_{RAN}. VERA greatly affected $I_{TTX,}$ but produced only minor changes on I_{RAN}, probably because of the presence of different subpopulations of VGSC, differently affected by the drugs.
4) Besides I_{NaL}, I_{TTX} and I_{RAN} included a relevant outward component that was abolished in the presence of K-channel blockers. Such evidences demonstrated the presence of a Na-activated K^+ current (I_{KNa}).
5) Selective activation of I_{KNa} by bithionol greatly reduced the inward component of $I_{TTX,}$ demonstrating the functional coupling between I_{NaL} and I_{KNa}. Consistently, bithionol reverted the depolarization induced by VERA, suggesting that V_m is modulated by the equilibrium between I_{NaL} and I_{KNa} when the former is enhanced.
6) I_{KNa} presence was confirmed at the molecular level by the presence of both *SLACK* and *SLICK* transcripts. Furthermore, RT PCR analysis detected several VGSC isoforms, confirming the evidences in point 3.

7) TTX reduction of the amplitude of Ca^{2+} increments was voltage-dependent, suggesting that the impact of I_{NaL} on Ca_i is tightly linked to V_m dynamics. The maximum effect of TTX was recorded at 0 mV, where the inward peak of the mixed I_{NaL}/I_{KNa} current was found. Moreover, TTX accelerated the decay of Ca_i levels, as expected from an increase in the driving force for the Na/Ca exchanger (NCX).
8) Chronic exposure to high glucose increased both the outward and the inward component of I_{TTX} and I_{RAN}, suggesting that pathophysiologically relevant conditions may produce I_{NaL} enhancement, with subsequent increase of $I_{KNa.}$
9) Consistently with previous works, TTX and RAN had negligible effect on the glucose-stimulated insulin secretion (GSIS) in basal conditions. Acute I_{NaL} enhancement by VERA resulted in a strong increase of insulin secretion, as expected from an acute Ca_i increment following intracellular Na (Na_i) accumulation. This effect was blunted by TTX and reduced by RAN, demonstrating VGSC involvement in the entire process.
10) Chronic exposure to high glucose (33 mM) reduced the response to the glucose challenge, an effect similar to the chronic I_{NaL} enhancement by VERA, which abolished the response to glucose. Notably, the effects of chronic high glucose exposure were slightly ameliorated by concomitant exposure to RAN. These evidences point to the fact that I_{NaL} enhancement, albeit beneficial for GSIS for brief periods, may become a relevant cause for insulin secretion dysfunction on the long term.

Overall, the evidences in Chapter 2 demonstrate the relevancy of I_{NaL} and its enhancement in a cell type (pancreatic β cells) different from neurons or cardiac myocytes.

The pathological effects of I_{NaL} enhancement may roughly be divided into electrical and ionic derangements. Although the former represents a major issue in cardiac myocytes[1-3], in pancreatic β cells the net inward current provided by I_{NaL} is effectively counteracted by the activation of the outward Na^+ dependent K^+ current (I_{KNa}), thus limiting the I_{NaL}-induced alterations on the normal electrical activity elicited by secretagogue stimuli. However, since V_m is only one of the several factors affecting GSIS[4], the presence of I_{KNa} alone may not be sufficient to hamper the negative effects of I_{NaL} enhancement.

As demonstrated by TTX effect on Ca_i reported in Chapter 2, the net Na^+ influx consequent to I_{NaL} activation results in Ca_i overload, an effect shared with cardiac myocytes[4-6]. Since the effect of I_{Na} blockade in INS-1E cells was voltage-dependent, the functional interplay between I_{NaL} and I_{KNa} represent a major factor in modulating ionic (most relevantly Ca^{2+}) homeostasis. It is widely recognized that in pancreatic β cells the membrane oscillators, consequent to I_{KATP} closure, are strictly dependent from the concentration of glucose[4]. The direct consequence is that altered glycemic levels might involve the balance between I_{NaL}/I_{KNa}, and the consequent Ca^{2+} load, in a different extent, depending on the entity of the initial glucose stimulus. Depending on the levels reached by V_m, the presence of I_{KNa} might sort beneficial or detrimental effects. Whereas the former may be due to V_m hyperpolarization opposing I_{NaL} activation, the same hyperpolarization might maintain a high driving force for Na^+ entry

through VGSCs, worsening the Na_i overload. However, since NCX activity is also modulated by V_m values, the glycemia-dependent effects of the combined I_{NaL}/I_{KNa} currents on Ca_i might be even more complex.

An important finding, with translational significance, was I_{NaL} enhancement in a model of chronic hyperglycemia, suggesting a potential common role of I_{NaL} enhancement as a marker of cell stress in different cell types. One possible explanation supporting this theory is the established cause-effect link between reactive oxygen species (ROS) and I_{NaL} enhancement. Since ROS production is a widespread response to different stress in almost all cell types[7], I_{NaL} enhancement may represent one of the final effectors of functional cell damage.

It is also important to notice that both the inward and the outward components of I_{TTX} (and I_{RAN}) were increased by chronic exposure to high glucose, suggesting that in pathophysiologically relevant conditions I_{KNa} might follow I_{NaL} enhancement, as a protective mechanism trying to restore V_m 'normal' behavior. Such a mechanism has already been proposed in neurons, where I_{KNa} could play a protective role against acute hypoxia[8].

Whereas the acute effects of I_{NaL} enhancers (veratridine) on insulin secretion are consistent with the Na-dependent Ca^{2+} overload pattern, chronic enhancement of I_{NaL} results in the opposite effect on GSIS. This may be explained by an increase in cell apoptosis or by chronic insulin leakage, resulting in reduced response to glucose due to depletion of the stores. In any case, the severe impairment of GSIS following chronic I_{NaL} enhancement may ultimately be ascribed to Ca^{2+} overload, responsible for both apoptosis and insulin leak.

As previously reported (CIT), chronic exposure to high glucose had negative effects on GSIS, but with magnitude inferior to VERA. This may be accounted for the different enhancement of I_{NaL} induced by the two conditions, as well as different I_{KNa} and Ca_i response, although I_{NaL} is probably not the only mechanism participating in hyperglycemia-induced stress. Nevertheless, concomitant RAN exposure significantly ameliorated the response to glucose, suggesting that I_{NaL} is actually involved in hyperglycemic stress. However, RAN did not totally preserve the glucose response, suggesting the presence of at least one I_{NaL}-independent mechanism.

Translational considerations

The evidences found in Chapter 2 provide significant observations in terms of multi-organ and translational application to the clinic. The presence of I_{NaL} and the impact of its enhancement in pancreatic β cells provide at least one mechanistic interpretation of the beneficial effects of RAN reported in T2DM patients[9].

Furthermore, since I_{NaL} enhancement has already been associated with several pathological conditions relevant to clinic (angina, epilepsy, heart failure) the demonstration of its involvement in hormone secretion mechanisms opens the possibility to consider I_{NaL} enhancement a widespread response to cell stress, thus making its selective blockers useful therapeutic tools to improve the treatment of several diseases in clinical practice. In particular, since the I_{NaL} blocker ranolazine is already used in clinic for the treatment of angina[10] and has been shown to have anti-diabetic effects[9], particular attention should be paid regarding the involvement of I_{NaL} on the

ancillary pathologic conditions of T2DM, *ie* diabetic cardiomyopathy and neuropathy.

Besides I_{NaL}, the experiments presented in Chapter 2 unveiled the presence of a Na-activated K conductance (I_{KNa}). Although this current is poorly studied, functional coupling between I_{NaL} and I_{KNa} represents an important phenomenon modulating I_{NaL}-induced cell damage. Thus, better understanding of I_{KNa} and its coupling with I_{NaL} enhancement may provide new potential therapeutic strategies in the treatment of cardiac, neuronal and pancreatic disorders.

Reference List of Chapter 3

1. Coppini R, Ferrantini C, Yao L, Fan P, Del Lungo M, Stillitano F, Sartiani L, Tosi B, Suffredini S, Tesi C, Yacoub M, Olivotto I, Belardinelli L, Poggesi C, Cerbai E, Mugelli A. Late Sodium Current Inhibition Reverses Electro-Mechanical Dysfunction in Human Hypertrophic Cardiomyopathy. *Circulation*. 2012.

2. Lu YY, Cheng CC, Chen YC, Chen SA, Chen YJ. ATX-II-induced pulmonary vein arrhythmogenesis related to atrial fibrillation and long QT syndrome. *Eur J Clin Invest*. 2012;42:823-831.

3. Zaza A, Belardinelli L, Shryock JC. Pathophysiology and pharmacology of the cardiac "late sodium current.". *Pharmacol Ther*. 2008;119:326-339.

4. Rorsman P, Braun M. Regulation of Insulin Secretion in Human Pancreatic Islets. *Annu Rev Physiol*. 2012.

5. Qian C, Ma J, Zhang P, Luo A, Wang C, Ren Z, Kong L, Zhang S, Wang X, Wu Y. Resveratrol attenuates the na(+)-dependent intracellular ca(2+) overload by inhibiting h(2)o(2)-induced increase in late sodium current in ventricular myocytes. *PLoS One*. 2012;7:e51358.

6. Undrovinas NA, Maltsev VA, Belardinelli L, Sabbah HN, Undrovinas A. Late sodium current contributes to diastolic cell Ca2+ accumulation in chronic heart failure. *J Physiol Sci*. 2010;60:245-257.

7. Birben E, Sahiner UM, Sackesen C, Erzurum S, Kalayci O. Oxidative stress and antioxidant defense. *World Allergy Organ J*. 2012;5:9-19.

8. Hage TA, Salkoff L. Sodium-activated potassium channels are functionally coupled to persistent sodium currents. *J Neurosci*. 2012;32:2714-2721.

9. Chisholm JW, Goldfine AB, Dhalla AK, Braunwald E, Morrow DA, Karwatowska-Prokopczuk E, Belardinelli L. Effect of

ranolazine on A1C and glucose levels in hyperglycemic patients with non-ST elevation acute coronary syndrome. *Diabetes Care*. 2010;33:1163-1168.

10. Scirica BM, Morrow DA. Ranolazine in patients with angina and coronary artery disease. *Curr Cardiol Rep*. 2007;9:272-278.

APPENDIX – LIST OF ACADEMIC CONTRIBUTIONS

Abstracts:

- E. Ferramosca, I. Rivolta, M. Joechler, L. Pisoni, C. Corsi, E. Grandi, **R. Rizzetto**, B. Dal Pozzo, S. Severi, A. Santoro. (2011). Cardiac activity modification uremia-related: a rabbit model. Giornale Italiano di Nefrologia. 52° Congresso della Società Italiana di Nefrologia. Genova. 21-24 settembre 2011. vol. 28, pp. S-53 ISSN: 0393-5590

Participation to international meetings*:*

- M. Rocchetti, **R. Rizzetto**, M. Alemanni, L. Sala, L. Barile, V. Zambelli, S. Maggioni, L. Staszewsky, G. Mostacciuolo, R. Latini, A. Zaza. Prevention of myocardial remodeling by chronic I_{NaL} blockade in pulmonary hypertension. Biophysical Society 56th annual meeting – San Diego, CA, February 25-29, 2012.
- **R. Rizzetto**, M. Alemanni, L. Barile, L. Sala, G. Mostacciuolo, A. Zaza, M. Rocchetti. Functional ventricular remodeling induced by pulmonary hypertension. EWGCCE annual meeting – Oslo, Norway, September 17-19, 2011.
- L. Sala, L. Barile, M. Alemanni, **R. Rizzetto**, G. Mostacciuolo, A. Zaza, M. Rocchetti. Effects of I_{NaL} blockade on cardiac remodeling in a model of pulmonary hypertension. EWGCCE annual meeting – Oslo, Norway, September 17-19, 2011.

- M. Rocchetti, S. Marangoni, **R. Rizzetto**, L. Barile, C. Altomare, G. Mostacciuolo, A. Zaza. Chamber-specific effects of Chronic Hypoxia on the late sodium current and repolarization. EWGCCE annual meeting – Cologne, Germany, September 17-19, 2009.

Publications*:*

- Marangoni S, Di Resta C, Rocchetti M, Barile L, **Rizzetto R**, Summa A, Severi S, Sommariva E, Pappone C, Ferrari M, Benedetti S, Zaza A. A Brugada syndrome mutation (p.S216L) and its modulation by p.H558R polymorphism: standard and dynamic characterization. *Cardiovasc Res* 2011; 91:606-16.

ACKNOWLEDGEMENTS

In the end, there the acknowledgements come. From my point of view, acknowledgements should stay in the front line.
Yes, they are only few words, and probably not enough to tell everything that is coming in my mind now as I write them. Life cannot be explained in a so few space.. However, it is crucial for me to write these words, since without the people included in this page I couldn't do anything. And that's why I think that acknowledgements should stay in the front line.
The first person I must give thanks to is of course Marcella, because all has begun from her simple question 'Do you wish to start a PhD?', and her support was present throughout these years. I give thanks to Claudia and Marzia, who supported me from the beginning, Luca and Carlotta, who helped me a lot (especially in choosing beers, but not only), and of course thanks to prof. Antonio Zaza for giving me the opportunity to work and learn a lot, also in different places.
The most special person who helped me in the fight for this PhD deserves one line for herself, and she is Alice Villa. During these two years you crossed one of the worst period in your life, but with the help of everyone, you found the strength to endure and continue to hope. It is just like the song that we used to listen during the exps: now you see that Star too, and I know that you will reach it, as I will do. Because this world is ours, *now*!
Special thanks are for Ilaria Rivolta and prof. Miserocchi, who gave me the possibility to begin my real PhD even in a difficult period. I must remember also Matteo Mangoni, my Mentor, Pietro, Angelo and Steve, my fellows in my French adventure in Montpellier. I'd like to

thank also Arvinder Dhalla and Luiz Belardinelli, who gave me the one-in-a-life opportunity to work in their company, Ruth and Ming, who helped me a lot during the American stay. It was a short time, maybe, but those days will be never erased from my mind. Thank you a lot.

Le ultime righe è bene che le scriva in italiano e sono dedicate a mamma Mariella, papà Vari, Cristina e Andrea. In italiano non perché siano meno importanti, ma proprio perché non potrei scrivere ringraziamenti altrettanto efficaci in inglese. Come ricordarvi altrimenti, dato che solo in italiano posso scrivervi: grazie per tutto quello che avete fatto, detto, sostenuto e –anche, qualche volta- contrastato. Se sono arrivato dove sono ora, è anche vostro merito. Che altro dire? Ai genitori ricordo solo un'altra frase, scritta nei ringraziamenti di un'altra tesi, qualche anno fa.

'Io e Cristina saremo i vostri successi più grandi'. Aggiungiamo un altro mattone, forgiato con il sangue, il fuoco e l'onore. Aggiungiamocelo alla torre che porta al successo, rinnovando la promessa: crediamo nel futuro e resistiamo nel presente. E soprattutto teniamo salda la fede, perché Chi vede possa agire e aiutare ancora, come ha fatto per me in questi tre anni, e che non posso non ringraziare. Believe in the future, and persist in the present. In fondo, sono ancora valide le parole di Churchill:

This is not the end. It is not the beginning of the end, either.

This is only the end of the beginning

GRAZIE A TUTTI!!!